Acta Pharmaceutica Sinica B 2021;11(8):2243–2264

Chinese Pharmaceutical Association
Institute of Materia Medica, Chinese Academy of Medical Sciences

Acta Pharmaceutica Sinica B

www.elsevier.com/locate/apsb
www.sciencedirect.com

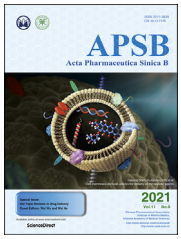

REVIEW

The reversed intra- and extracellular pH in tumors as a unified strategy to chemotherapeutic delivery using targeted nanocarriers

Edgar Pérez-Herrero[a,b,c,*], **Alberto Fernández-Medarde**[d]

[a]*Departamento de Ingeniería Química y Tecnología Farmacéutica, Universidad de La Laguna, La Laguna 38206, Tenerife, Spain*
[b]*Instituto Universitario de Bio-Orgánica Antonio González, Universidad de La Laguna, La Laguna 38206, Tenerife, Spain*
[c]*Instituto Universitario de Tecnologías Biomédicas, Universidad de La Laguna, La Laguna 38200, Tenerife, Spain*
[d]*Instituto de Biología Molecular y Celular Del Cáncer, Centro de Investigación Del Cáncer (USAL-CSIC), Salamanca 37007, Spain*

Received 2 November 2020; received in revised form 11 December 2020; accepted 4 January 2021

KEY WORDS

pH-Gradient inversion;
Metabolism of glucose;
Proton transport inhibitors;
Proton-caged carriers;
Chemotherapy;
Targeted drug delivery;
pH-Sensitive nanocarriers;
Warburg effect;
Cancer

Abstract Solid tumors are complex entities, comprising a wide variety of malignancies with very different molecular alterations. Despite this, they share a set of characteristics known as “hallmarks of cancer” that can be used as common therapeutic targets. Thus, every tumor needs to change its metabolism in order to obtain the energy levels required for its high proliferative rates, and these adaptations lead to alterations in extra- and intracellular pH. These changes in pH are common to all solid tumors, and can be used either as therapeutic targets, blocking the cell proton transporters and reversing the pH changes, or as means to specifically deliver anticancer drugs. In this review we will describe how proton transport inhibitors in association with nanocarriers have been designed to block the pH changes that are needed for cancer cells to survive after their metabolic adaptations. We will also describe studies aiming to decrease intracellular pH in cancer using nanoparticles as molecular cages for protons which will be released upon UV or IR light exposure. Finally, we will comment on several studies that have used the extracellular pH in cancer for an enhanced cell internalization and tumor penetration of nanocarriers

*Corresponding author.
E-mail address: eperezhe@ull.edu.es (Edgar Pérez-Herrero).
Peer review under the responsibility of Chinese Pharmaceutical Association and Institute of Materia Medica, Chinese Academy of Medical Sciences.

https://doi.org/10.1016/j.apsb.2021.01.012

and a controlled drug delivery, describing how nanocarriers are being used to increase drug stability and specificity.

1. Introduction

From old, humanity has search for a miracle cure for all diseases, a pill that cures it all. This has also been true in the search for a general treatment for cancer. Unfortunately, the term "cancer" comprises a vast amount of diseases, developed through the accumulation of a varied set of genetic alterations, making every patient unique[1,2]. This has forced healthcare professionals to use a battery of individual therapeutic strategies for each type of cancer, but in spite of this individualized approach, and because of their genetic heterogeneity, every patient will have a different response to the treatment, and many will die due to the illness. Notwithstanding their genetic heterogeneity, all liquid and solid tumors have many features in common, which are related to the physiological, biochemical and molecular mechanisms that lead to the initiation of the tumor, its progression and metastasis[3]. These shared characteristics are known as the hallmarks of cancer, and include: deregulated proliferation, apoptosis avoidance, escape from the immune system, the acquisition of an invasive phenotype, induction of angiogenesis, obtaining replicative immortality, securing of an inflammatory environment, genetic instability and altered cell energetics[4]. These common features may allow us to search for a unified strategy that could allow to fight against cancer as a whole. Indeed, several therapeutic strategies have already been used to target some of those hallmarks: drugs that block proliferation or inhibit angiogenesis have been used in the clinic for years[5], and the approach to enact an immune response against tumors has seen a revolution in the last ten years[6]. In spite of these advances, many cancers are still incurable, and for those, the cure might be found among the other hallmarks.

In this regard, Otto Warburg discovered almost 100 years ago a common and unique characteristic of solid tumors that differentiate them from the normal tissue. Cancer cells show an abnormal metabolic behavior in which the metabolism of glucose through the glycolytic pathway to lactate has a predominance over the degradation through the tricarboxylic acid (TCA) cycle and oxidative phosphorylation. These metabolic changes are now considered a hallmark of cancer, an adaptation necessary for tumor development[4]. In healthy cells, in the presence of physiological levels of oxygen, TCA cycle and oxidative phosphorylation are the main pathways used to degrade the pyruvate generated through glycolysis, because they are the most efficient metabolic pathways to obtain adenosine triphosphate (ATP) from glucose (36/38 ATPs per glucose). Cellular metabolism in cancer shift glycolysis to generate lactate from pyruvate (which is known as "aerobic glycolysis"), in order to adapt to the hypoxic conditions found in many tumor areas (Pasteur effect), because this metabolic pathway is able to produce energy in the absence of normal levels of oxygen. Recently, this notion has been proved to be partially wrong, since aerobic glycolysis is also observed in the presence of oxygen in tumor cells. This raises an obvious question: why is this aerobic glycolysis chosen by the tumor cells despite being so inefficient (only 1 ATP per glucose)? The answer is speed: aerobic glycolysis is almost 100 times faster than complete degradation of glucose by TCA cycle and oxidative phosphorylation. In addition, aerobic glycolysis is thought to be necessary to complement the oxidative phosphorylation in order to fulfill the increased energetic demands of highly proliferative cancer cells[7]. This metabolic shift must be necessary for tumor initiation because the appearance of the aerobic glycolysis is an early event in the oncogenic transformation[8]. In these initial stages of tumor development, the change to this metabolic route might be facilitated by the role of several oncogenes that are increasing glucose metabolism[9]. This is the case for the *RAS* GTPases, oncogenes mutated in a 30% of human malignancies, which activate PI3K signaling, a key regulator of glycogen degradation, glucose uptake and expression of glycolytic enzymes such as hexokinase 2 and phosphofructokinase 1 (Fig. 1). In addition, activating mutations in *PI3K* or deleterious mutations in the tumor suppressor *PTEN* (a negative regulator of this pathway) are frequent events in cancer. Another oncogene that is implicated in the control of glycolysis is MYC. This transcription factor, overexpressed in many cancers, is known to induce the expression of pyruvate kinase or lactate dehydrogenase (*LDHA*), thus activating the aerobic glycolysis (Fig. 1)[10]. As already mentioned, aerobic glycolysis might be an additional mechanism to obtain energy for tumor cells when normal oxygen levels are present but is a necessity in tumor areas where the access to oxygen is scarce. In hypoxic conditions, cancer cells adapt their metabolism through the expression of hypoxia inducible factor (HIF1). This protein induces the expression of most enzymes regulating the normal glycolytic pathway, as well as *LDHA* in the aerobic glycolysis. In addition, it inhibits pyruvate dehydrogenase avoiding pyruvate degradation *via* TCA cycle and oxidative phosphorylation and, thus increasing its transformation to lactate[10].

As a consequence of the metabolic shift in cancer, the degradation of glucose in malignant cells by aerobic glycolysis will lead to the production of large amounts of lactic acid and a concomitant increase in proton (H^+) concentration inside the cancer cells. For this reason, in order to avoid the apoptotic response that would induce this acid stress, malignant cells use several mechanisms to extrude this excess of H^+ from the cytoplasm by plasma membrane-bound proton transporters and proton pumps that are upregulated in tumors, provoking a decrease of the tumor extracellular pH (pH_e) and a concomitant increase of the intracellular pH (pH_i)[11] (Fig. 1). The increase in pH observed inside the cancer cells is not only produced by the overexpression of H^+ extrusion systems, but also because of the decrease in the CO_2 production consequence of the reduction of the TCA cycle and oxidative phosphorylation[11]. Intracellular alkalinity helps avoid apoptosis, induces an increase in the proliferation of malignant cells through induction of G2/M transition and is directly related to the development of multiple drug resistance (MDR). Moreover, acidic pH_e promotes invasion and metastasis, and increases MDR, angiogenesis and tumor immune escape[8,12–14].

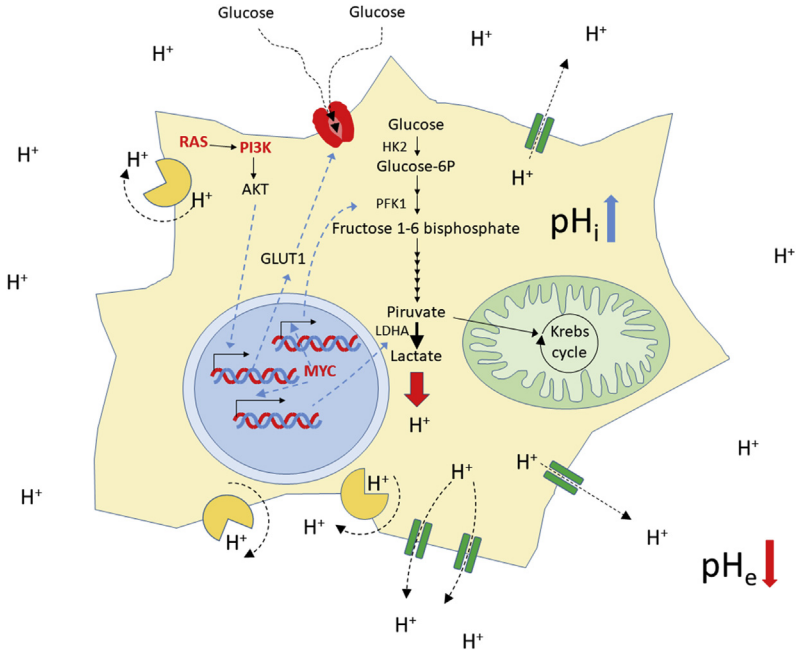

Figure 1 An increase in aerobic glycolysis to lactate in the tumor cells leads to an accumulation of protons that are actively removed from the cell by proton pumps (in light orange) and transporters (green). This activity produces an accumulation of protons in the extracellular media and a concomitant pH increase at the cytosol. The augmented glycolytic flux is driven by the action of several oncogenes (in bold red letters), that induce the expression and activation of most of the glycolytic enzymes. For a comprehensive review on the role of oncogenic signals in the control of glycolysis see reference 9. HK2: hexokinase 2; PFK1: phosphofructokinase 1; LDHA: lactate dehydrogenase A; GLUT1: glucose transporter 1; pH_i: intracellular pH; pHe: extracellular pH.

As already mentioned, the altered pH of the cancer cells has a positive impact on the development of many cancer hallmarks. Thus, the inversion of this reverse pH gradient ($pH_i > pH_e$) in tumors is being used to design promising new treatments in cancer. Some of the approaches used to date tried to induce acid stress inside the cancerous cells in order to force apoptosis either by a) inhibition of the proton extruder systems, b) increasing lactic acid production with molecules that diminish the mitochondrial activity, c) inducing lysosomal membrane permeabilization or d) generating intracellular acidification with non-proton acidifiers or light-activated proton carriers[8,11,15]. Other interesting approaches take advantage of the slightly acidic extracellular microenvironment of tumors for drug delivery, using cytotoxic substances and/or carriers that are more active and/or change its physical−chemical properties at the pH_e[16]. As mentioned above, extracellular acidification favors tumor dissemination and other laboratories have aimed to revert this abnormal pH_e as a therapeutic approach[17]. Finally, the overexpressed proton pumps in tumors can be the basis for targeted therapies in cancer, either by their direct inhibition or as molecular identifiers of the tumoral cells that could be used for recognition in the delivery of cytotoxic drugs[18].

Nanocarriers have been commonly used as vehicles of anticancer agents in indirect targeted therapies. Their custom design allows their specific accumulation and/or release in tumors, bypassing normal tissues, which highly reduces drug toxicity and provides protection from degradation. It also increases several-fold drug accumulation in the tumors, allowing the use of lower drug concentrations. In addition, nanocarriers reduce the mononuclear phagocyte system (MPS) clearance and improves the control over the release kinetics[19]. Moreover, nanocarriers can be designed to take advantage of the pH-centric paradigm and use this as a unified strategy to fight against cancer, regardless of the pool of genetic alterations in the tumor. In this review, we will analyze in detail some of the late developments in nano-scale carriers that aim to take advantage of the abnormal intra- and extra-cellular pH in tumors for targeted therapies.

2. Proton transport inhibitors and nanocarriers

Proton transport in the cells is the key in the regulation of numerous physiological functions. In addition to maintaining the intracellular pH in the physiological values (≈7.2), they are also used to generate electrical and chemical gradients needed for the transport of metabolites, and the proton accumulation, generated by the electron transport chain in the inner membrane of the mitochondria, is used to generate ATP by the ATP synthase[20,21].

Malignant cells overexpress different plasma membrane-bound proton transporters (PTs) and proton pumps (PPs, Tables 1–4), such as Na^+/H^+ exchanger-1 (NHE1), monocarboxylate-H^+ co-transporters or MCTs (mainly MCT1 and 4 isoforms), carbonic anhydrases or CAs (mainly CA9 and CA12 isoforms), bicarbonate transporters (mainly Na^+/HCO_3^- co-transporters or NBCs) and vacuolar ATPase proton pumps (V-ATPases)[22,23]. These up-regulated proton extruder systems avoid intracellular acidification and therefore apoptosis in cancer cells, inducing alkalinization of the cytoplasm (to ≈ pH 7.4) and extruding the excess of protons to the extracellular environment that changes from pH 7.4 in normal tissues to pH 6.5−7.0 in tumors. Although these

Table 1 Vacuolar ATPases in cancer.

Cancer	*ATP6V0A1*	*ATP6V0A2*	*ATP6V0A3 TCIRG1*	*ATP6V0A4*	*ATP6V0B*	*ATP6V0C*	*ATP6V0D1*	*ATP6V0D2*	*ATP6V0E1*	*ATP6V0E2*	*ATP6V1A*	*ATP6V1B1*	*ATP6V1B2*
Adrenal gland	16.46	**20.25**	n/a	11.39	n/a	10.13	**75.95**	11.39	**32.91**	11.39	7.59	13.92	10.13
Breast	5.53	6.61	4.44	3.89	4.8	8.33	3.99	0.36	7.32	4.89	3.89	3.53	0.18
CNS	3.73	4.73	5.6	1.87	3.44	3.16	5.88	2.3	4.02	10.9	4.3	3.87	4.16
Cervix	2.93	0.33	4.89	2.28	8.14	3.58	0.98	4.89	4.23	4.23	**20.85**	2.61	6.19
Endometrium	5.15	6.98	4.65	2,82	6.48	10.47	4.65	2.16	4.82	6.31	5.32	8.8	5.32
Hematop. & Lymph.	2.71	5.88	5.88	5.43	2.71	2.26	9.95	2.26	4.52	3.62	3.62	4.07	4.98
Kidney	5.83	5.17	8	3.5	3.5	2.67	4.67	2.67	1.83	6.33	2.67	3.17	2.83
Large intestine	7.38	6.23	3.28	4.26	4.59	5.74	6.39	5.74	4.59	13.44	3.93	4.1	1.97*
Liver	8.04	7.77	9.12	6.7	4.29	5.36	2.41	5.09	11.26	7.24	5.9	6.17	1.61
Lung	2.45	4.32	2.45	6.48	6.77	6.28	4.61	2.45	5.4	8.24	13.74	5.79	1.57
Oesophagus	4	11.2	1.6	4.8	8	2.4	3.2	0.8	8[a]	6.4	10.4	2.4	4
Ovary	1.5	6.02	3.76	3.76	10.15	1.5	2.26*	1.88	5.64	6.02	10.9	7.89	2.63[b]
Pancreas	7.82	3.91	1.68	2.23	3.35	3.91	8.94	3.35	2.79	4.47	4.47	3.35	2.79
Prostate	3.01	4.82	4.82	2.81	6.22	5.02	4.82	2.81	4.82	7.63	4.02	3.41	3.21
Skin	4.44	5.07	3.17	0.63	6.55	5.29	1.69	2.33	4.02	9.09	4.23	1.06	2.75
Soft tissue	6.08	4.56	1.14	1.52	7.22	9.51	2.66	2.28	3.42	4.94	3.04	3.04	1.52
Stomach	8.42	6.67	5.26	3.51	7.02	6.67	8.77	5.96	5.26	3.86	3.86	5.26	14.74
Thyroid	3.51	3.7	2.34	0.58	3.9	7.8	8.77	1.95	5.46	2.92	3.9	3.12	1.75
Upper aerodig. tract	3.07	7.09	6.13	2.11	5.94	5.75	5.75	3.26	4.6	3.07	12.64	1.15	2.87
Urinary tract	2.94	5.39	1.72	3.19	5.39	2.94	5.15	3.92	3.19	9.31	8.09	0.98	1.72

Cancer	*ATP6V1C1*	*ATP6V1C2*	*ATP6V1D*	*ATP6V1E1*	*ATP6V1E2*	*ATP6V1F*	*ATP6V1G1*	*ATP6V1G2*	*ATP6V1G3*	*ATP6V1H*	*ATP6AP1*	*ATP6AP2*	*VMA21*
Adrenal gland	13.92	5.06	2.53	n/a	1.27	8.86	10.13	1.27	n/a	10.13	15.19	**34.18**[a]	**41.77**
Breast	**24.55**	8.24	4.44	3.53	8.42	6.43	4.62	6.7	1.45	**20.47**	6.97	4.26	12.14
CNS	4.59	5.02	4.3	4.45	5.31	6.17	3.3	3.59	1.72	4.16	3.59	2.73	5.16
Cervix	**21.82**	6.19	5.54	4.23	9.12	6.84	3.58	11.07	1.3	12.05	14.98	17.26	**21.82**
Endometrium	17.94	4.82	4.65	7.52	10.3	6.98	2.94[a]	12.62	1.5	13.95	9.63	8.14	7.48
Hematop. & Lymph.	7.69	5.43	3.62	6.33	4.52	2.71	5.88	6.33	2.26	4.98	4.52	4.98	7.24
Kidney	2.67	1.83	2.67	3.83	5.83	2	2.67	2	1.67	3	10.67	7.17	9.83
Large intestine	**31.15**	8.85	2.13	5.41	6.56	9.51	6.39	3.61	0.33	**21.31**	**21.48**	18.2	**22.3**
Liver	**39.41**	10.46	4.56	6.43	7.51	9.65	4.29[a]	6.97	n/a	19.57	**23.59**	4.83	16.89
Lung	**23.36**	5.5	6.58	8.44	9.03	9.91	5.99	3.14	3.24	11.68	9.03	6.77	17.08
Oesophagus	**31.2**	10.4	4	8	7.2	4	12	14.4	12.8	12[a]	9.6	5.6	8.8
Ovary	**35.71**	6.77	4.14	10.15[a]	19.92	7.52	5.64[a]	12.03	7.52	15.04	8.65	4.89	12.41[a]
Pancreas	11.17	6.7	5.59	8.38	4.47	6.15	5.59	1.68	3.91	6.7	12.29	10.06[a]	9.5
Prostate	16.67	3.41	4.22	5.62	5.02	9.04	8.63	3.21	1.61	8.63	n/a	n/a	n/a
Skin	11.21	3.81	2.11	5.71	4.02	9.3	2.96	8.03	6.13	8.25	4.44	4.86	9.94
Soft tissue	5.32	3.04	4.94	3.42	3.04	3.04	3.42	9.51	5.32	2.28	15.21	**26.62**	8.37
Stomach	**30.18**	6.67	5.96	10.53	5.26	9.47	12.63	5.26	8.42	**26.67**	**22.81**	11.93	8.77
Thyroid	4.29	4.29	5.07	2.92	4.87	4.48	3.51	4.87	4.09	6.04	5.26	3.9	4.29
Upper aerodig. tract	**20.11**	2.68	7.47	7.85	10.15	4.79	10.34	2.11	3.26	12.45	10.34	6.9	19.73
Urinary tract	**26.23**	7.35	5.39	9.56[a]	6.62	6.13	1.96	2.94	2.45	12.5	**23.53**	10.29	11.52

Overexpression levels of the vacuolar ATPase family members in cancer affecting several tissues.
Overexpression >20% in bold letters.
n/a, not available.
Asterisks: also downregulated in some patients.
[a](5%−10%).
[b](10%−15%).

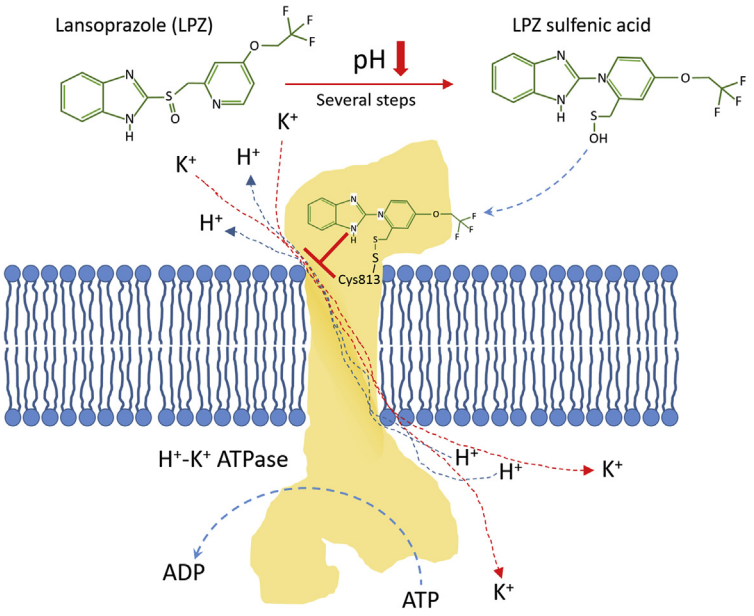

Figure 2 Mechanism of action of lansoprazole. In acidic environments the sulfoxide residue in lansoprazole is transformed into a sulfenic acid, which can bind to cysteine 813 in the ATPase and inhibit proton transport to the stomach lumen. These inhibitors can be used in cancer to block acidification of the tumor microenvironment, but also to induce a reduction in intracellular pH that would lead to cell death.

changes of pH look small, they have a huge impact in the cells and their environment[20,21], and blocking these PTs and PPs is a promising therapeutic approach that is currently being exploited as an anti-cancer strategy (Supporting Information Table S1)[23]. Moreover, since an acidic pH_e increases MDR reducing the therapeutic efficacy of antineoplastic drugs, the use of proton transport inhibitors (PTIs) and proton pump inhibitors (PPIs) might be a good option as an adjuvant strategy to improve the effects of chemotherapy[11].

2.1. *Vacuolar ATPases (V-ATPases) inhibition*

V-ATPases are proton pumps that use ATP hydrolysis to provide energy for H^+ transport from the cytoplasm to the lumen of internal compartments or the extracellular media. They are used in normal cells for acidification of lysosomal lumen, transport of metabolites, etc. In cancer, V-ATPases have been described to play a role in tumor microenvironment acidification, and an elevation of V-ATPase levels has been associated with increased invasion and metastasis. V-ATPases are overexpressed in many types of cancer[24] (Table 1). Specifically, the *ATP6V1C1* gene is highly expressed in many human cancers, especially liver (overexpressed in almost 40% of the cases), ovary (35,6%) or colorectal (31%). Also, increased expression levels from the genes *ATP6V1H*, *ATP6AP1*, *ATP6AP2* and *VMA21* have also been found in several tumors (Table 1). In addition, V-ATPases are commonly targeted to the plasma membrane in tumors[24], and these transporters are needed for signaling through several important pathways in tumor progression, such as WNT, NOTCH and MTOR[21,25–27].

Some drugs, like lansoprazole, pantoprazole, esomeprazole, omeprazole and rabeprazole are PPIs that block the gastric H^+-K^+ ATPases and are currently being used in the treatment of acid-related disorders[28]. In fact, Alai et al.[29–31] developed different nanoparticulate oral delivery systems for the sustained release of lansoprazole (LPZ) all day long in the treatment of gastric ulcers and to avoid nocturnal acid secretions. These authors prepared positively charged LPZ-loaded nanoparticles (NPs) based on the non-biodegradable and bio-adhesive Eudragit RS100 and the oil-in-water (o/w) emulsion solvent evaporation method. They also formulated negatively charged LPZ-NPs using poly (lactic-*co*-glycolic acid) (PLGA) and the double emulsion (w/o/w) solvent evaporation method. Both formulations showed *in vitro* and *in vivo* sustained release profiles for up to 24 h and healing values higher that 90% in gastric ulcers in rats after 7 days of daily oral administration.

Since the above-mentioned PPIs are prodrugs that accumulate easily in acidic environments where they become active, they will show no toxicity until activated in the extracellular milieu of the tumor, differentiating them from the majority of the anticancer drugs that are inactivated in the acidic extracellular pH in tumors[28]. In fact, numerous preclinical studies and some ongoing clinical trials can be found in the literature about the usefulness of these PPIs to increase the pH_e and avoid MDR in cancer[17,23,32]. Paškevičiūtė and Petrikaitė[33] reported the use of two PPIs, omeprazole (OPZ) and lansoprazole (LPZ), to enhance delivery of doxorubicin in its free form or inside PEGylated liposomes to 4T1 breast cancer cells and 3D cell cultures (4T1) at simulated pH_e of 6.0, not observing this effect at physiological pH and being LPZ more effective than OPZ.

Among all the V-ATPase inhibitors, lansoprazole (LPZ) has shown the best anti-tumor efficacy[34] and an enhanced sensitivity to chemotherapeutic agents, like paclitaxel (PTX)[35] or doxorubicin (DOX)[36] (Fig. 2). Bhattacharya et al.[37] selected the optimal formulation parameters using the Box-Behnken design to include PTX and LPZ in PLGA-based NPs prepared by the double emulsion solvent evaporation method (Fig. 3). They were able to include both drugs in the formulation by using a 7:3 ratio (*v*/*v*) of dichloromethane/ethanol mixture in the organic phase. pH 8.0 and 20 °C were maintained during the preparation of the NPs to address the sensitivity of LPZ to both variables. After the statistical optimization, the selected formulation exhibited a "mean size" of 243.7 nm, encapsulation efficiencies and drug loading

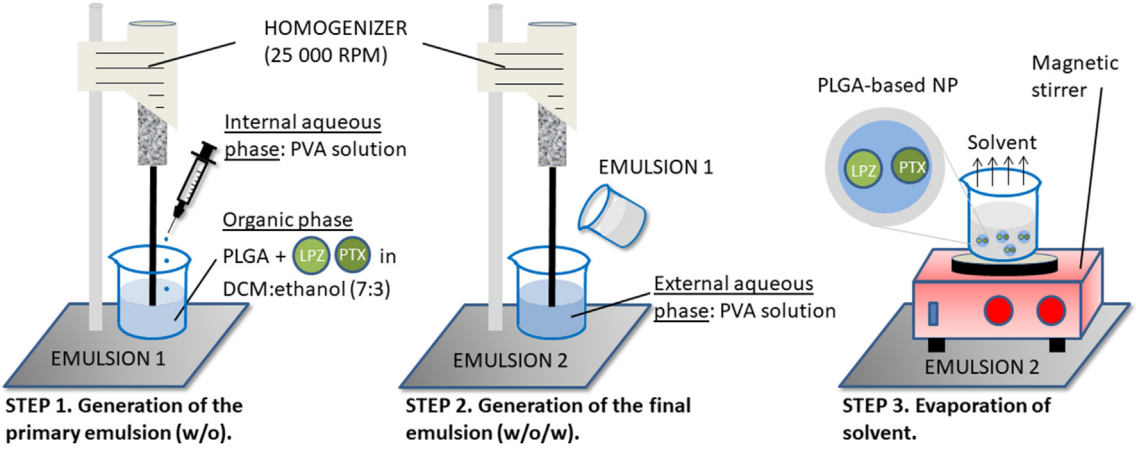

Figure 3 Preparation protocol of paclitaxel (PTX) and lansoprazole (LPZ) loaded PLGA-based NPs by the double emulsion solvent evaporation method. The use of LPZ as PPI in combination with the protection provided by the PLGA-based NPs reduces the PTX resistance.

values for both drugs higher than 80% and 40%, respectively, and a controlled release of PTX and LPZ over 384 h, following a Fickian diffusion. The PTX-LPZ-loaded PLGA NPs produced a higher decrease in the cell viability of MCF7 breast cancer cells when compared with the combined free drugs after 48 and 72 h. The authors justified the enhanced cytotoxicity of the encapsulated PTX and LPZ because of high concentrations of both drugs inside the cells, due to the rapid uptake of NPs, and controlled release profiles produced by the diffusion of the drugs across the polymer matrix.

Despite the advantages of using targeted nanocarriers in combination with V-ATPase inhibitors to enhance the delivery of weakly basic chemotherapeutic agents, to the best of our knowledge, apart from the reports by Paškevičiūtė[33] and Bhattacharya[37] (Table S1), no other papers have been published in this regard.

2.2. Na^+/H^+ exchangers (NHE) inhibition

The SLC9A solute carriers is a family of Na^+/H^+ exchangers (NHE) implicated in the control of intracellular pH and cell proliferation. It is comprised of nine members, but only NHE1 is ubiquitous and is thought to have a central role in the movement of protons through the plasma membrane in most tissues and cell

Table 2 Na^+/H^+ exchangers (NHE) in cancer.

Cancer	*NHE1*	*NHE2*	*NHE3*	*NHE3R1*	*NHE3R2*	*NHE4*	*NHE5*	*NHE6*	*NHE7*	*NHE8*	*NHE9*
Adrenal gland	n/a	**22.78**	1.27	2.53	8.86	15.19	5.06	**35.44**	11.39	**32.91**[b]	2.53
Breast	2.54	5.62	5.89	15.49	7.88	1.9	3.8	10.14	5.89	15.49	3.35
CNS	4.59	4.59	4.45	4.73	3.59	6.31	3.73	6.31	2.58	7.03	4.3
Cervix	3.58	3.58	4.56	7.17	2.93	1.63	9.45	22.8	6.31	8.79	11.07
Endometrium	3.16	3.16	4.32	3.82	5.48	3.65	9.3	5.81	8.47	8.31	3.65
Hematop. & Lymph.	4.07	1.36	3.62	4.07	4.07	5.43	6.33	4.07	4.52	4.07	2.71
Kidney	4.33	3.33	5.67	4	6.33	0.83	7	7.33[a]	8[a]	4.17	5
Large intestine	2.46	4.92	5.57	4.26	7.05	3.28	7.05	12.46	9.84	**24.92**	4.1
Liver	3.22	2.95	3.22	16.89	2.95	3.49	5.36	15.28	8.58	5.36	3.75
Lung	2.36	7.16	4.32	4.91	3.53	5.4	6.38	9.62	8.73	5.4	10.11
Oesophagus	7.2	4	4	10.4	2.4	3.2	**25.6**	6.4	1.6	**44.01**	10.4
Ovary	1.5	3.38	13.53	7.52	2.26	7.52	0.38	8.65	3.38	5.64	1.13
Pancreas	3.35	9.5	5.59	6.15	6.15	6.7	4.47	12.29	1.12	6.15	4.47
Prostate	3.82	4.82	2.21	5.22	5.62	4.62	3.01	n/a	n/a	3.41	6.22
Skin	4.44	0.85	7.61	2.75	2.96	2.96	9.73	7.4	16.28	14.8[a]	2.54
Soft tissue	6.84	6.08	1.52	3.04	2.28	3.8	4.56	0.76	18.25	12.93	6.46
Stomach	4.56	11.93	11.23	7.37	5.26	7.72	5.96	6.32	11.93	16.84	2.46
Thyroid	3.51	3.12	0.19	3.9	5.46	0.58	1.95	4.87	3.31	2.53	3.51
Upper aerodig. tract	5.56	3.07	4.98	6.13	5.75	2.87	5.56	7.85	4.6	5.75	10.92
Urinary tract	4.17	8.82	3.92	5.39	4.17	9.8	7.84	3.92	6.13	11.76	2.7

Overexpression levels of the Na^+/H^+ exchanger (NHE) family members in cancer affecting several tissues.
Asterisks: also downregulated in some patients.
Overexpression >20% in bold letters.
n/a, not available.
[a](5%−10%).
[b](10%−15%).

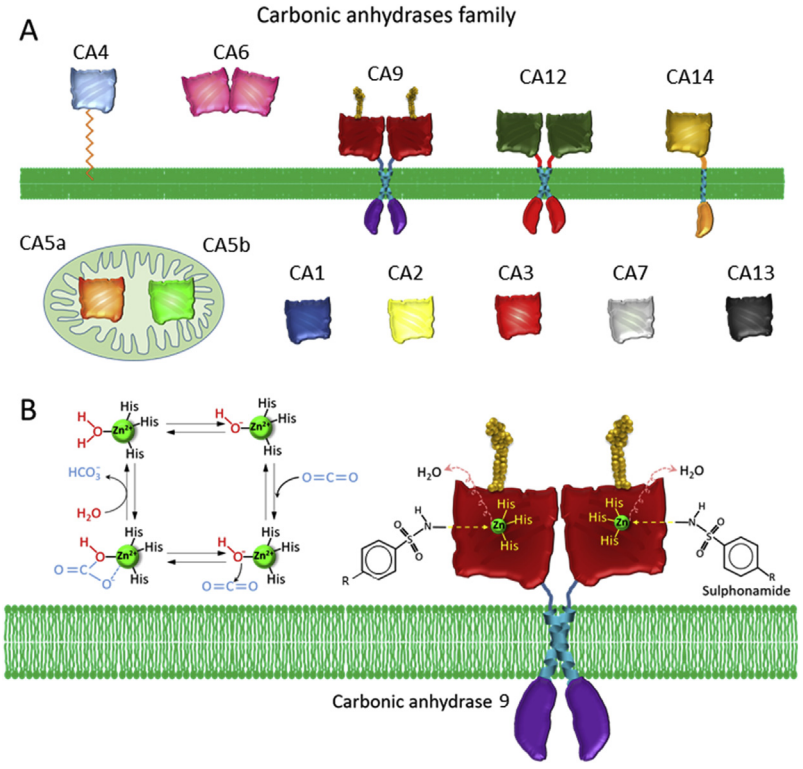

Figure 4 Carbonic anhydrases (CAs) as possible molecular targets in cancer treatment (A) The family of the carbonic anhydrases comprise several members located either at the plasma membrane, in the cytosol or in the mitochondria. Among these pH regulators, *CA9* and *CA12* seem to have an important role in cancer, where they are usually overexpressed (B) Mechanism of action of sulphonamides in CA inhibition. CAs need a zinc residue bound to three histidines for the catalytic reaction. Sulphonamides bind to this zinc atom and displaces a molecule of water that is needed for the transformation of CO_2 into NCO_3^-.

types. NHE2-5 are also plasma membrane transporters, but their role is limited to specific tissues, meanwhile NHE6-9 are located in intracellular organelles. The importance of NHE1 in overall pH regulation is emphasized by its role in cancer. In fact, to date, among this family only NHE1 has been clearly implicated in tumor formation and dissemination, and its elimination blocks tumor growth in nude mice, marking it as a possible therapeutic option in cancer[38–40]. Despite the absence of published work regarding the implication of other members of this family in cancer, a search on the COSMIC database[41] for alterations in *NHE* expression in cancer showed that *NHE8* gene is overexpressed in many esophagus tumors, where 44% of the samples tested showed NHE-8 overexpression (Table 2). Note that, although the implication of NHE1 is well established in literature[38–40], low rates of overexpression are shown in Table 2, which can be explained because of the low amount of data compiled for this gene in COSMIC. Unfortunately, the only NHE1 inhibitor to reach clinical trials, cariporide, had to be removed due to its cardiotoxicity[20,32,42].

2.3. *Monocarboxylate-H^+ co-transporters (MCTs) inhibition*

Monocarboxylate−H^+ co-transporters (MCTs) link the transport of protons and several metabolites through the plasma membrane. Each transporter is specific for one or several metabolites and has an important role in the regulation of cellular processes and metabolic pathways such as gluconeogenesis, thyroid hormone metabolism, T-cell activation, etc. Among these transporters, *MCT1* and *MCT4* have shown a clear pattern of overexpression in many types of cancer, where they function as regulators of the lactate metabolism promoting the metabolic changes observed in cancer as well as inducing angiogenesis and cell migration[43]. Table 3 shows the overexpression rates for the members of the *MCT* family in several types of cancer[41]. Despite the apparently low overexpression rates shown in the COSMIC database for the individual *MCT*s in individual types of cancer, the added overexpression of the members of this family in cancer is very high, stressing their importance in pH regulation in tumors[43].

The overexpression of these transporters can be used as a therapeutic target to specifically deliver chemotherapeutic agents inside nanocarriers towards the cancer cells (Table S1). In fact, Calori et al.[44] prepared 100 nm alpha-cyano-4-hydroxycinnamic acid (CHCA)-coated liposomes by the ethanol injection method, where CHCA acts as ligand to target MCT1 in MCF-7 and U-87 MG cancer cells and reduces oxidative stress because of their antioxidant properties. The authors reported an enhanced uptake of the carriers over the control in MCF-7 (26%) and U-87 MG (63%) cell lines using a concentration of CHCA of 50 μmol/L. Moreover, they demonstrated the antioxidant properties of CHCA, including aluminum chloride phthalocyanine in the liposomes as photosensitizer. In this way, they produced *in situ* oxidative stress in the cells by laser irradiation at 670 nm and they measured the decrease in cell death in the presence of CHCA.

Moreover, several pharmaceutical companies have developed inhibitors for MCTs, although only AZD3965, a MCT1 inhibitor, is now in clinical trials[20,32,45–47]. Huang et al.[48] prepared 33 nm

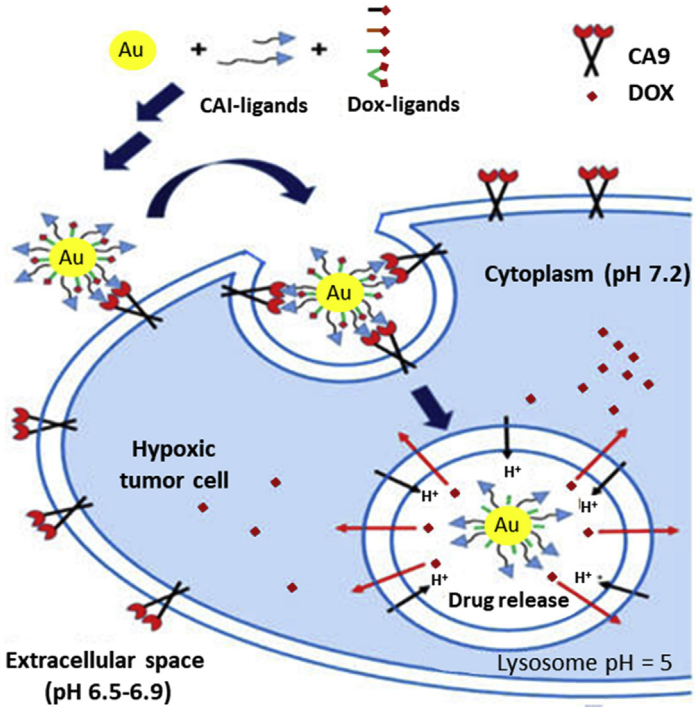

Figure 5 Scheme of PEGylated CAI-conjugated Au-NPs for a pH-dependent and selective intracellular delivery of DOX. Reprinted with modifications by permission from Ref. 60. Copyright © 2018 American Chemical Society.

AZD3965-loaded PEG-*b*-(poly (dipropylaminoethyl) methacrylate) (PDPA) micelle nanoparticles (AZD-PDPA NPs) generated by nanoprecipitation method with microfluidics to inhibit MCT1 in cancer cells and reduce tumor immune evasion. The pH-sensitive characteristics of the system permitted the targeted delivery of all the MCT1 inhibitor contained in the carrier, which remained intact in blood circulation at physiological pH, until it reached the tumor, where the extracellular acidic pH (pH_e) generated their immediate release because of the disassembly of the carriers. The authors demonstrated the protection of the drug within the AZD-PDPA NPs at physiological pH and the similar activity of free AZD3965 and AZD-PDPA NPs (with acidic pre-treatment) in TC-1 cancer cells by measuring the presence of lactate and the variation of pH in the extracellular medium. Intravenous administration (i.v.) of AZD-PDPA NPs at a very low dose in TC-1 and B16F10 melanoma animal models showed an enhanced tumor growth inhibition (1.5-fold) over the oral administration of free AZ3965 at the recommended dose (>200 times the i.v. dose within the AZD-PDPA NPs), reducing cardiac and liver toxicities.

2.4. *Carbonic anhydrases (CAs) inhibition*

Carbonic anhydrases (CAs) are zinc metalloproteinases used by the cells to eliminate protons and CO_2. This elimination is especially important in cancer where there is an accumulation of both H^+ and CO_2 due to the enhanced glucose metabolism. Overexpression of several CAs has been observed in cancer, specifically *CA9* and *CA12*. *CA9* expression is induced by HIF1 and blocking its activity leads to tumor growth inhibition[49] (Fig. 4A).

These high expression levels of *CA9* are reflected in the data found at the COSMIC database[41], where *CA9* is found overexpressed in a third of upper aerodigestive tract and ovary cancers (Table 4), but also, in the GEO profile dataset[50], *CA9* overexpression is observed in studies analyzing cervical, squamous lung and metastatic prostate cancer. Moreover, there are few genomic studies of *CA9* in kidney cancer, where its importance has been established in several individual studies[51]. In addition, other CAs, such as *CA5B* and *CA10*, are overexpressed in adrenal gland and ovary tumors, respectively (Table 4).

Several inhibitors aiming to block CAs (CAIs) have been developed. Among them, several immunotherapy approaches against *CA9* have reach as far as phase III clinical trials and might be the first cancer therapies targeting proton transporters to reach the clinical practice[47]. Moreover, recent publications have shown the effectiveness of sulfonamide CAIs (Fig. 4B), like the classical acetazolamide and dorzolamide, or the compounds SLC-0111 and indisulam that have reached phase II clinical trials[32,42,47,52].

Some authors have used *CA9* as therapeutic target to achieve a selective delivery of chemotherapeutic agents toward cancer cells by using conjugates (Table S1). Krall et al.[53] reported the first small molecule−drug conjugate to specifically deliver cytotoxic drugs to tumors overexpressing *CA9*. They used 5-amino-1,3,4-thiadiazole-2-sulfonamide (CL 5343), an acetazolamide derivative, as *CA9* ligand to achieve the targeted delivery of maytansinoid to the cell membrane of SKRC52 renal cancer cells. The authors showed the efficient tumor accumulation of CL 5343-fluorescent dye conjugates (13.4% of injected dose per gram of tissue, % ID/g, in 1 h) when applied to mice bearing subcutaneous tumors. Moreover, a non-toxic dose of 70 nmol of CL5343-maytansinoid conjugates showed a potent antitumor activity in those mice, compared to the standard treatment of kidney cancer with sunitinib and sorafenib. In a similar approach, Cazzamalli et al.[54] reported acetazolamide-monomethyl auristatin E conjugates with a potent antitumor activity in mice bearing SKRC52

Table 3 Monocarboxylate-H^+ co-transporters (MCTs) in cancer.

Cancer	*MCT1*	*MCT2*	*MCT3*	*MCT4*	*MCT5*	*MCT6*	*MCT8*	*MCT9*	*MCT10*	*MCT11*	*MCT12*	*MCT13*	*MCT14*
Adrenal gland	1.27	**29.11**	1.27	2.53	**29.11**	3.8	2.53	1.27	2.53	10.13	3.8	8.86	**20.25**
Breast	6.79	2.9	1.36	8.33	2.99	5.53	7.7	2.54	4.35	3.35	2.36	7.34	4.62
CNS	4.45	3.59	5.02	4.88	5.6	4.45	5.02	3.16	2.58	4.43	2.15	4.02	3.16
Cervix	4.89	1.63	2.93	5.54	2.28	3.58	8.47	10.42	3.58	2.61	3.91	3.58	1.63
Endometrium	5.15	3.16	5.65	4.32	6.31	4.49	6.31	8.64[a]	9.47	5.15	4.98	7.14	6.64
Hematop. & Lymph.	2.26	5.43	2.26	4.52	11.31	4.07	5.43	**21.72**	4.52	4.98	4.52	3.17	3.17
Kidney	6.37	3	2.17	5.17	3.75	3.67	3.83	3.64	3.67	14.5	6	13.33	4.67
Large intestine	2.79	3.93	3.11	4.26	6.39	8.69	6.56	4.43	3.93	3.11	5.25	1.15	3.11
Liver	4.02	3.49	3.22	6.43	6.43	6.43	8.04	2.14	3.22	3.49	6.97	0.8	2.41
Lung	4.91	3.73	5.4	6.87	2.75	5.5	2.45	4.22	2.85	1.08	2.65	11.19	8.15
Oesophagus	6.4	5.6	9.6	0.8	0.8	9.6	12	3.2	5.6	1.6	11.2	10.4	10.4
Ovary	18.05	2.26	3.01	12.03	6.77	**22.18**	6.39	6.39	6.77	1.88	12.41	**28.95**[b]	4.14
Pancreas	2.76	3.35	9.5	5.59	6.15	6.15	2.79	10.06	2.79	9.5	7.82	11.17	6.15
Prostate	3.41	5.02	0.4	4.82	2.41	3.61	n/a	5.22	5.62	4.82	4.42	1.2	5.22
Skin	6.34	4.65	1.9	5.5	2.96	5.29	2.75	2.75	2.33	7.61	1.48	5.29	0.85
Soft tissue	3.42	1.9	0.76	4.94	1.52	4.18	5.7	4.36	9.89	2.66	2.28	4.94	9.13
Stomach	6.32	10.18	8.42	7.02	7.37	6.67	4.21	8.07	8.07	14.39	4.21	11.23	4.91
Thyroid	3.12	3.51	1.95	4.29	3.12	4.29	6.04	3.9	5.85	3.31	4.29	4.09	4.29
Upper aerodig. tract	5.36	3.26	2.49	4.79	1.15	6.7	10.15	4.02	4.6	3.26	2.68	7.09	6.13
Urinary tract	9.59	4.17	1.96	6.62	5.64	7.6	2.21	7.35	1.72	3.19	0.49	7.35	3.43

Overexpression levels of the monocarboxylate-H^+ co-transporter (MCT) family members in cancer affecting several tissues.
Asterisks: also downregulated in some patients.
Overexpression >20% in bold letters.
n/a, not available.
[a](5%−10%).
[b](10%−15%).

renal carcinomas. Among different dipeptide linkers analyzed, valine−alanine and valine-citrulline showed the best stability *in vitro* (half-life of 23 and 11.2 h, respectively) and antitumor efficacy *in vivo*. Likewise, Marks et al.[55] synthesized a conjugate for the targeted delivery of the cytotoxic tubulysin B towards *CA9* expressing tumor cells. To do that, they used the *CA9* inhibitor fluoro-benzosulfonamide (CAL) previously reported by Dudutiene et al.[56] that possessed the best specificity and affinity values for *CA9* of all the inhibitors tested by the authors. The CAL-fluorescein isothiocyanate (FITC) conjugates showed a potent binding capacity to the cell membrane of HT29, SKRC52 and A549 *CA9* expressing cancer cells. In addition, these authors

Table 4 Carbonic anhydrases (CAs) in cancer.

Cancer	CA1	CA2	CA3	CA4	CA5A	CA5B	CA6	CA7	CA8	CA9	CA10	CA11	CA12	CA13	CA14
Adrenal gland	1.27	1.27	1.27	5.06	3.8	**56.96**	7.59	12.66	5.06	12.66	0	2.53	3.8	1.27	**49.37**
Breast	1.27	2.26	0.82	2.36	4.98	6.61	0.27	6.34	8.97	5.89	0.36	2.54	3.26	6.52	8.06
CNS	3.01	2.87	1.87	2.15	3.16	5.31	1.29	4.88	3.01	6.46	5.88	5.45	5.45	4.59	11.19
Cervix	1.3	4.89	5.21	1.95	1.95	2.28	2.93	0.33	3.58	8.14	1.95	4.23	6.19	4.56	10.1
Endometrium	3.32	5.65	7.81	2.49	2.49	3.16	3.65	5.32	4.82	9.47	3.65	11.63	3.49	5.65	6.24
Hematop. & Lymph.	4.98	4.52	2.71	4.07	8.6	1.81	3.17	11.31	8.14	4.62	8.14	7.24	2.26	5.88	6.33
Kidney	4.17	1.17	1.5	4.5	4.5	7.83	5.67	0.67	3.67	1.5	1.17	5	5	2.83	3.67
Large intestine	4.26	3.11	12.79	7.05	3.61	3.11	1.64	1.64	3.93	5.08	3.28	5.41	3.44	12.79	2.95
Liver	1.07	4.29	0.8	4.56	1.88	6.97	4.02	5.36	1.34	4.83	2.14	2.95	4.29	6.7	7.77
Lung	2.75	2.65	3.83	1.47	2.45	3.73*	0.39	4.32	4.22	4.61	4.61	9.13	4.12	8.73	3.73
Oesophagus	8	8	4	10.4	0.8	0.8	9.6	14.4	8.8	n/a	6.4	8.8	2.4	8.8	**35.2**
Ovary	6.02	2.26	4.51	1.88	1.5	1.5	8.27	6.39	14.29	**28.95**	**24.81**	3.01	3.76	2.26	18.05
Pancreas	1.12	3.91	2.79	1.12	4.47	3.35	1.68	1.12	3.91	14.53	4.47	9.5	5.03	7.26	6.7
Prostate	2.41	4.22	1	2.81	4.82	n/a	1.61	6.83	6.22	5.42	1	5.42	4.02	4.42	2.61
Skin	1.69	2.75	3.81	2.96	3.59	3.17	1.9	2.54	5.5	4.86	2.11	4.02	6.55	8.67	13.32
Soft tissue	1.52	2.66	0.38	7.22	4.56	12.93	0.76	5.7	3.04	4.94	1.9	2.28	4.56	0.76	0.38
Stomach	5.61	5.61	4.56	6.67	1.05	7.72	3.86	12.63	3.86	3.16	6.32	11.93	6.32	10.88	3.16
Thyroid	0.39	0.19	0.78	4.87	2.53	3.12	1.56	7.41	0.19	4.68	1.56	6.04	5.85	2.73	3.51
Upper aerodig. tract	1.34	11.88	2.87	0.57	0.38	5.56	3.45	2.49	3.64	**33.52**	4.21	5.56	4.41	4.02	7.47
Urinary tract	1.72	1.72	4.41	7.11	0.98	4.66	0.74	0.98	3.68	4.9	3.92	6.37	3.43	4.41	5.15

Overexpression levels of the carbonic anhydrase (CA) family members in cancer affecting several tissues.
Asterisks: also downregulated in some patients. * (5%−10%), ** (10%−15%). Overexpression >20% in bold letters. n/a, not available.

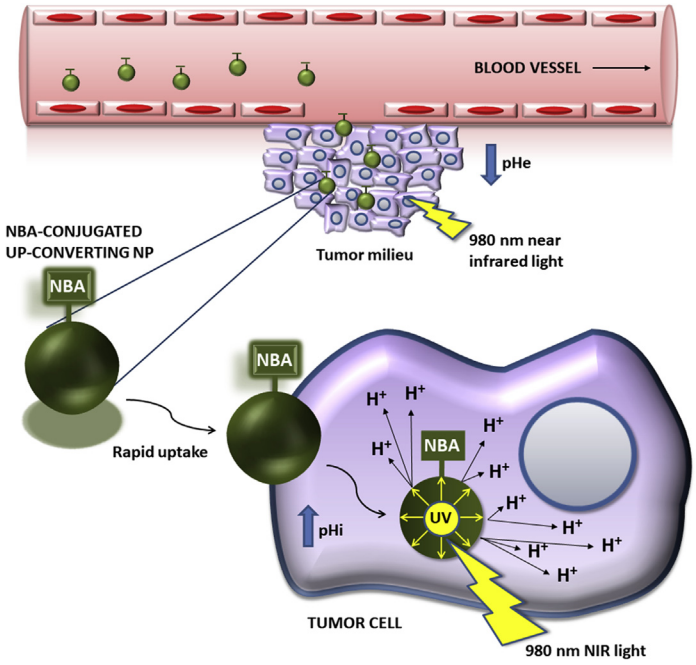

Figure 6 Mechanism of action of NBA-conjugated up-converting NPs. They absorb low-energy NIR light (980 nm) and emit high-energy UV light (350−400 nm) to generate intracellular acidification by the cleavage of NBA and the consequent release of protons inside the cancerous cell.

demonstrated the efficacy of CAL-tubulysin B conjugates (with self-immolative linkers) in killing transfected HEK293 cells (IC_{50} = 1.05 nmol/L) and reducing HT29 tumor xenografts in mice and A549 tumor xenografts in mouse with no toxicity. Lv et al.[57] reported the synthesis of *CA9* inhibitor-containing conjugates, with a PEG linker, to the specific delivery of tubulysin B or technetium-99 m to *CA9* expressing cancer cells. The authors chose the potent *CA9* inhibitor polyamino-polycarboxylamido aromatic sulfonamide, previously reported by Rami et al[58]. Biodistribution studies in mice bearing HT-29 tumor xenografts showed that the CA9 inhibitor-technetium-99 m conjugates markedly accumulate in tumor with a low % ID/g of 1.4 ± 0.4 after 4 h. The *CA9* inhibitor−tubulysin B conjugates showed an IC_{50} value of 4.4 nmol/L in HT-29 cancer cells with no toxicity up to concentrations of 1 μmol/L and an absence of growth of the tumor in mice bearing HT-29 xenografts after the administration of the non-toxic dose of 2 μmol/kg.

Apart from the *CA9* ligand−drug conjugates, there are other carriers that can specifically deliver cytotoxic drugs to *CA9* expressing cancer cells (Table S1).

Janoniene et al.[59] developed 185 nm porous silicon nanoparticles (NPs) functionalized with VD11-4-2, a sulfonamidic fluorescent CA inhibitor (CAI) synthesized by the authors, for the targeted and pH-sensitive delivery of doxorubicin (DOX) to MCF-7 breast cancer cells. The system showed a potent affinity, specificity and killing capacity for *CA9* expressing MCF-7 cells.

Shabana et al.[60] described for the first time PEGylated CAI-conjugated Au-NPs that target *CA9* isoform for delivery of DOX to hypoxic tumor microenvironments (Fig. 5). In order to selectively reach the transmembranal *CA9* isoform, these authors combined membrane-impermeable oligoethyleneglycol (3 units) or PEGylated (with a low molecular weight of 2000) *CA9* inhibitor conjugates, as targeting ligands, with Au-NPs, which are also impermeable to the plasma membrane. The optimized formulation, which contained the best ligand density and the maximum drug loading in the surface of the particles to maintain colloidal stability, was very effective against HT-29 tumor cells under hypoxic conditions. Moreover, this formulation enhanced 2.5 times the intratumoral delivery of DOX when compared with non-targeted formulations or free DOX, minimizing chemoresistance. In order to achieve a selective delivery of DOX to the lysosomes of cancer cells, these authors studied the influence of the length of the spacer between the particles and the ligands to avoid the nonspecific uptake of the CAI-conjugated Au-NPs under hypoxic conditions. The Au-NPs with PEG spacers avoided the unspecific uptake observed in Au-NPs or CAI-conjugated Au-NPs with short spacers under normoxic or hypoxic conditions. Based on that, they showed the influence of the level of oxygen on the uptake of CAI-conjugated Au-NPs when PEG spacers were used, observing a low uptake under normoxic conditions and a high *CA9*-mediated uptake under hypoxia. The optimum conjugation of DOX to the surface of the Au-NPs was achieved by a conjugate of DOX with dithiodipropionic acid (DTDP), as anchoring ligand, and hydrazone, as pH-dependent linker. This synthesis strategy led to a pH-dependent release profile of DOX, with a controlled release of less than 25% at pH 7.4 after 24 h and a burst release of 80% and 98% after 4 and 24 h, respectively, at an acidic pH of 5.5.

Alsaab et al.[61] reported an 159.5 nm acetazolamide-conjugated micellar nano-formulation based on vitamin-E-α-D-tocopherol (TPGS) and styrene maleic anhydride (SMA) to specifically deliver the apoptosis inducer CFM 4.16, in combination with sorafenib, to the hypoxic core of the tumor, in order to overcome the MDR in renal cell carcinoma (RCC). The authors showed the capacity of the formulation to produce a large decrease in cell viability of everolimus-resistant (Evrm-res) A498 renal cancer cells (IC_{50} = 850 nmol/L) compared to free everolimus (IC_{50} >10 μmol/L) and sorafenib (IC_{50} = 9 μmol/L), showing a synergistic killing effect when combined with low doses of sorafenib. In addition, they demonstrated the great hypoxia-mediated penetration of *CA9*-targeted TPGS-SMA oligomers in the core of

Evrm-res A498 RCC cells-based tumor spheroids and tumors of mice bearing subcutaneous Evrm-res A498 RCC (3-fold compared to control and 2-fold compared to peripheral tissue of tumor) by near infrared imaging. Moreover, they demonstrated the enhanced antitumor capacity of the formulation in combination with sorafenib, in Evrm-res A498 tumors, compared to the treatment with the free drugs, with no toxicity in liver and kidney.

Recently, Tatiparti et al.[52,62] reported the targeted delivery of 3,4-difluorobenzyliden curcumin (CDF)[52] or paclitaxel (PTX)[62] to *CA9* expressing MDA-MB-231 and MDA-MB-468 triple negative breast cancer (TNBC) cells by means of acetazolamide-conjugated albumin NPs, which were prepared by the desolvation/coacervation method and the copper-free click chemistry. According to the cytotoxic studies, the CDF or PTX-loaded systems showed an enhanced efficacy in killing TNBC cell lines (IC_{50} of 31.13 or 1 μmol/L of CDF or PTX for MDA-MB-231 and 3.78 or 0.5 μmol/L of CDF or PTX for MDA-MB-468) compared to the non-targeted system and the free cytotoxic drugs, being the percentage of living cells up to 2.8 times lower in the case of hypoxic conditions with respect to normoxic conditions[52,62]. The authors explained these results by an enhanced hypoxia-mediated internalization of the acetazolamide-conjugated NPs in *CA9* overexpressing cells, which was demonstrated by fluorescent cell uptake studies, and the enhanced apoptotic capacity of the *CA9*-targeted system with respect to the non-targeted one[52,62]. In addition, the injection of the acetazolamide-conjugated albumin NPs, modified with a near infrared dye, into mice bearing TNBC patient-derived tumor xenografts showed their specific accumulation in the tumor, with a reduced uptake in the spleen and the liver[52].

The high affinity of the classic CAIs for all the different isoforms of the CAs has reduced their advance to clinical use since they produce inhibition of CAs in normal cells and not only in the targeted CAs[20,47]. Thus, to avoid the toxic side effects of most of these inhibitors, new approaches have been developed to design more selective inhibitors in order to reduce the deleterious effects to the normal tissue. CAs are located and distributed differently depending on their isoform, being in particular *CA9* and *CA12* the only membrane-bound isoforms that generate their catalytic activity in the extracellular milieu[11]. Taking advantage of this fact, several authors have designed different strategies to avoid the passage of CAIs throughout the plasmatic membrane, preventing their interaction with the intracellular CA isoforms.

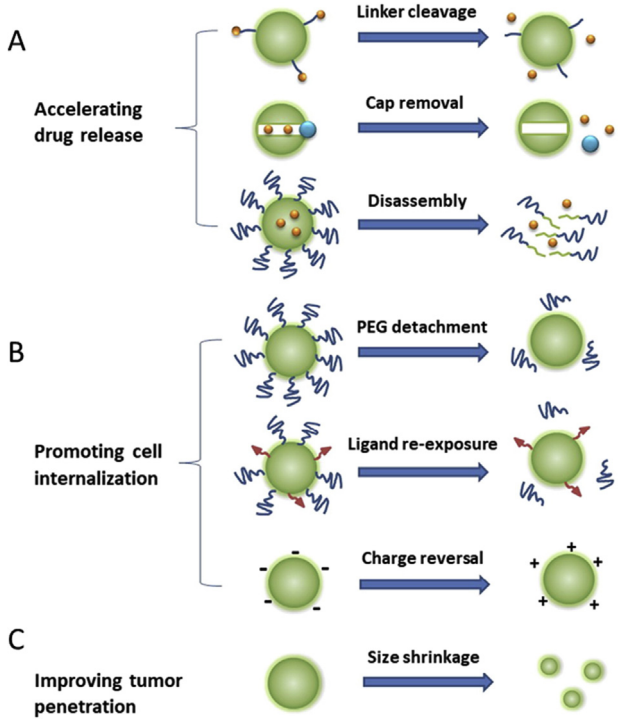

Figure 7 Mechanisms of action of pH-sensitive nanocarriers. Reprinted from Ref. 92. Copyright © 2015 with permission from Elsevier.

In this regard, gold nanoparticles (Au-NPs) have played an important role. Stiti et al.[63] synthesized CAI-coated Au-NPs with an average particle size of 3.3 nm and non-permeable characteristics with respect to the plasmatic membrane. They showed promising comparative data about several CAIs, the standard acetazolamide, the sulfonamide 3a and the sulfonamide-3a-coated Au-NPs. As controls, they used a sulfonamide derivative with no CAs inhibition, either isolated or coating the Au-NPs, and non-coated Au-NPs, showing no inhibition of any of the isoforms. Acetazolamide showed inhibition of the CA2 and 9 isoforms, however, the sulfonamide 3a, either isolated or coating the Au-NPs, showed a good selectivity in the inhibition of the *CA9* isoform over *CA1* and *2*, presenting the best selectivity when coating the Au-NPs due to their membrane-impermeable characteristics. New work on this formulations[64] improved the synthesis route of the CAI-coated Au-NPs by a one-pot modified citrate method to achieve dispersibility and stability in aqueous media, maintaining the selectively to inhibit the transmembrane isoforms *CA9* and *12* over the cytosolic CA1 and 2. This new approach achieved very stable aqueous colloidal suspensions, where the CAI coating of the Au-NPs, a sulfonamide derivative, played an important role in the stabilization of the Au-NPs when increasing the ionic strength. The authors concluded that the inhibition is only due to the interaction between the sulfonamide derivative and the CAs, contributing the Au-NPs in the selectivity towards the membrane-bound isoforms because of the impermeability of the particles to the plasmatic membrane.

Ratto et al.[65] proposed for the first time the use of plasmonic gold nanorods with dog-bone shapes and sulfonamide derivatives as a combined therapy in cancer to achieve a selective inhibition of the transmembrane CA isoforms and near infrared (NIR) hyperthermia. The authors showed the *in vitro* specific accumulation of the CAI-conjugated gold nanorods in human colorectal carcinoma HCT116 and human mammary adenocarcinoma MDA-MB-231 cells under hypoxic conditions. The incorporation of CAIs to the gold nanorods produced a clear cytotoxic effect that is directly related to the inhibition of the transmembrane CAs. In fact, cytotoxicity was stronger in the MDA cells than in the HCT, since the mammary cells express *CA9* only while the HCT116 cells show activity of the *CA9* and *12* isoforms. The specific inhibition of the *CA9* and *12* by the CAIs-conjugated gold nanorods was confirmed by a partial alkalinization of the extracellular environment. A large reduction in cellular proliferation was observed, but induction of apoptosis was similar to the administration of the CAIs alone. When the CAIs-conjugated gold nanorods were excited at the low power density of 50 W/cm^2, the combined effect of optical hyperthermia and CAs inhibition was lethal to the cells under hypoxic conditions. As mentioned before[60], in addition to the generation of hyperthermia, the gold nanorods added impermeability to the plasmatic membrane to get a selective and

targeted inhibition of the membrane-bound CA isoforms in the cancer cells.

3. Nanocarriers for intracellular proton release

An innovative approach to reverse the anomalous pH gradient in tumors is the direct generation of intracellular acidification by proton-caged carriers that may initiate an apoptotic pathway in cancerous cells remotely *via* UV irradiation. A caged compound is a molecule that is trapped in an inactive form, normally by a chemical conjugation with light-sensitive linkers, and is released as an active form when irradiated with near-UV light that break the spacer, removing the protecting group[66]. This technology has been used in cancer therapy to achieve a controlled delivery of anticancer drugs, like 5-fluorouracil (5-FU), avoiding the toxicity of the drug outside the tumor. Agasti et al.[67] reported 2 nm 5-FU-conjugated Au-NPs, using ortho-nitrobenzyl (ONB) as the photo-cleavable linker between the drug and the surface of the particles. These authors monitored the 5-FU controlled release from the Au-NPs when irradiated with UV-light (365 nm) that cleaved the ONB. Drug release was only observed under irradiation, with a maximum value after 10 min. Thus, the 5-FU-conjugated Au-NPs did not produce cytotoxicity in MCF-7 cells in the dark, but when particles were irradiated for 20 min a strong decrease in cell viability was observed. The authors demonstrated the promising properties of Au-NPs as carriers and cages of anticancer drugs that are inactive when linked to the particles and produced the required therapeutic effect when released after exposure to UV-light.

The majority of the reported caged compounds are built with a 2-nitro-benzyl or 2-nitro-phenyl linker and one proton is released when these conjugates are irradiated with UV-light to liberate the trapped molecule in their active form, generating a rapid acidification[68]. Taking advantage of these facts, some compounds that include photo-sensible moieties, such as 2-nitro-benzyl or 2-nitro-phenyl, have recently been developed as proton caged carriers (PCC) to generate photo-inducible intracellular acidification. This is achieved by means of protons that are released because of the ionization of nitronic acid, the primary phytochemical product that is generated by the photolysis of the 2-nitro benzyl or 2-nitro-phenyl-based compounds[68]. Furthermore, these PCC are normally modified to be conjugated to different nanocarriers in order to facilitate their internalization and thus generate the intracellular acidification.

Carbone et al.[69] demonstrated by FTIR spectromicroscopy the possibility of reducing the pH_i of NIH 3T3 fibroblast cells by using the synthetic PCC 1-(2-nitrophenyl)-ethylhexadecyl sulfonate (HDNS) and UV irradiation at 275−375 nm. Based on this compound, they synthesized a new PCC, the disulfanediyldinonane-9,1-diylbis{[1-(2-nitrophenyl)ethoxy]sulfonyl} carbamate (NESS-deca) that contains the light-sensitive *o*-nitrobenzoic ester but also includes sulfur groups to allow its conjugation to the surface of 22 nm Au-NPs[70]. HEK-293 cells were incubated with free NESS-deca or NESS-deca-conjugated AuNPs and, following the CO_2 signal by FTIR spectroscopy they monitored intracellular acidification after UV irradiation. The conjugation of NESS-deca to the AuNPs enhanced 400 times their acidification capacity inside the cells due to the improved cellular uptake of the PCC because of the vectorial properties of AuNPs.

In a similar approach, Sabbatella et al.[71] synthesized the di-sulfanediyldiesane-6,1-diylbis{[1-(2-nitrophenyl)ethoxy]sulfonyl}carbamate (NESS-hepta) and the above-mentioned NESS-deca. Both compounds, which possessed the *o*-nitrobenzyl photo-cleavable group to generate acidification and the disulphide group to be conjugated to 22 nm Au-NPs, were characterized by FTIR and ^{1}H NMR. The acidification capacity of both compounds was assessed by FTIR spectroscopy after UV-irradiation and their conjugation ability to Au-NPs by thermo-gravimetric analysis (TGA).

Gdovin et al.[15] used the PCC *o*-nitrobenzaldehyde (NBA) and UV irradiation to generate a significant intracellular acidosis that induced apoptosis of different cell lines in 2 h. Thus, the reduction of pH_i induced an 85% apoptotic rate in the non-cancerous rat pheochromocytoma PC12 cells and a 98% rate in breast cancer MCF-7 cells. The apoptosis values in MCF-7 cells under UV light or NBA alone were significantly lower (7.1% or 2.3%) than a combination of NBA and UV-based irradiation. Moreover, they described that NBA diffuses easily into the cell and remains trapped and inactive until irradiated with UV-light, at which time it generates intracellular acidification, independently of the cell line, being this combination effective in inducing apoptosis in non-cancerous PC12 cells, MCF-7 and MDA-MB-231 human breast cancer cell lines, BxPC-3 human pancreatic cancer cell line and LNCaP human prostate cancer cell line. *In vivo*, they performed the treatment of triple negative breast cancer in mice with NBA and UV-irradiation, resulting in a significant reduction of the tumor volume and growth, as well as an increase in the survival of the animals. In addition, these authors made an important contribution to this therapeutic strategy by conjugating NBA to up-converting NPs (UPNPs) in order to solve the difficulty of reaching deep tissue regions with near UV irradiation (350−550 nm). UPNPs are able to absorb low-energy near infrared (NIR) light at 980 nm that easily penetrate in biological tissues without causing damage and emit the high-energy photons at 350−400 nm that are necessary to produce the cleavage of NBA and generate the intracellular acidification (Fig. 6). The reported NBA-conjugated UPNPs produced similar intracellular acidification and apoptotic cell death (91.5%) than using NBA and UV-irradiation and can be functionalized to target cancer-specific receptors. Using a similar approach, Zhou et al.[72] recently reported the assembly of poly (amidoamine) (PAMAM) dendrimers on the surface of polyacrylic acid (PAA)-coated UPNPs to include in the system the PCC capacity of NBA. These 80 nm NBA-PAMAM-PAA-UPNPs were able to release hydrogen ions to generate intracellular acidification in HN3T3 cells and HepG2 cancer cells by the emission of photons of 365 nm with irradiation at 980 nm.

4. pH-sensitive drug nanocarriers

The main drawbacks of chemotherapy are the growth inhibition and unspecific damage on normal cells, which produces important side effects in the patients[19]. One of the most frequent approach to maintain chemotherapeutic drugs inactive and apart from blood circulation until located in the tumor microenvironment, is the use of nano-scale carriers.

In this section, we describe the use of the reverse pH gradient and the consequent acidic extracellular microenvironment in tumors to generate a focalized delivery of anticancer drugs. Several approaches use the acidic extracellular pH (pH_e) to induce a pH-dependent drug release (Fig. 7A) by:

(1) The destabilization of the structure of drug-loaded nanocarriers, which are elaborated including pH-sensitive moieties, like poly (histidine), poly (aspartic acid-graft-

imidazole), poly (beta-aminoester) or diethylaminopropyl, that possess a destabilization pH ranged between 6.5 and 6.8, below which reversible hydrophobic/hydrophilic transitions or swelling occur, which induce drug release from nanocarriers (see section 4.1.1).

(2) The destabilization of the shell of the pores of drug-loaded silica NPs that are coated by pH-sensitive compounds, like poly (histidine), poly (2-pentamethylenimino) ethyl methacrylate or crosslinked chitosan, whose alteration at pH_e induces the release of the drug included inside the pores of the carriers (see section 4.1.2).

(3) The hydrolysis of the 2,3-dimethylmaleic anhydride acid-labile linker included in the nanocarrier at the extracellular tumoral pH (pH_e) that provoke the release of the drug by the breakage of the initial electrostatic interactions between the drug and the system (see section 4.1.3).

Thus, pH-responsive carriers act as vehicles of these toxic agents while in circulation, avoiding the contact with normal cells, till they reach the acidic tumor milieu that activate the release of the cargo. In addition to its use to destabilize the nanoparticles, the acidic tumoral environment can be used to promote the cell internalization of the carriers (Fig. 7B) by several approaches:

(1) pH-Induced surface charge modifications in the carriers from negative at physiological pH, that increases their blood circulation, to positive at pH_e, that induces their intracellular uptake. This is achieved by including in the composition of the nanocarriers different pH-sensitive compounds, like polysulfadimethoxine, poly (histidine) and 2,3-dimethylmaleic anhydride and derivatives (see section 4.2.1).

(2) The use of pH-sensitive structures, like the benzoic-imine linker, the Pro-Leu-Gly-Val-Arg peptide sequence conjugated to poly (aspartic acid) or the poly (histidine) block, that allow to hide the active targeting ligands conjugated to the surface of the nanocarriers at the physiological pH to prolong their blood circulation, and permit the ligand appearance at pH_e to activate the intracellular uptake at the tumor site (see section 4.2.2).

(3) The inclusion of pH-sensitive PEG chains in the nanocarriers through the conjugation of PEGylated structures that contains 2,3-dimethylmaleic anhydride and allow their detachment at pH_e, while provide blood circulation at physiological pH (see section 4.2.3).

Finally, tumor penetration of nanocarriers can be promoted by decreasing their size below 30 nm at the acidic pH_e, using pH-sensitive blocks, like poly (2-azepane ethyl methacrylate) or polycaprolactone, to overcome the poor vasculature and dense extracellular matrix in tumors (Fig. 7c).

4.1. *pHe-induced drug release*

4.1.1. *Structural destabilization of nanocarriers*

One of the methods to deliver the content of the nanocarriers in the tumor area is to use the acidic pH of the tumor environment to induce a destabilization of the nanocarriers. This is usually achieved by using pH sensitive structures that change their characteristics at a pH below the physiological value. In the following lines we will describe the main strategies used to date for this purpose (Supporting Information Table S2).

An approach frequently used has been to include pH-sensitive blocks, mainly poly (histidine) and poly (beta-aminoester) (PAE), in the structure of the polymers that will later form part of the delivery systems. When the pH-sensitive drug carrier reaches the tumor, the slightly acidic pH_e (6.5−7.0) destabilizes the polymers causing the release of the content of the carrier.

This strategy was used for the first time by Bae and collaborators, who developed polymeric micelles based on poly (L-histidine)-*b*-poly (ethylene glycol) and poly (L-lactide)-*b*-poly (ethylene glycol). Poly (histidine) pH-sensitive blocks generated the destabilization of the micelles under acidic conditions due to reversible transitions from a hydrophobic state at pH values above 7.4 to a hydrophilic state by protonation of amine groups at pH values below 7.0[73]. Varying the ratio between both polymers, these authors were able to optimize the sensitivity of the micelles. A 25% (*w*/*w*) of poly (L-lactide)-*b*-poly (ethylene glycol) led to the destabilization of the micelles at pH 6.8, being stable at pH values ranged between 7.0 and 7.4. Using this formulation they observed an increase in the cumulative release of adriamycin from 32% (*w*/*w*) at pH of 7.0−70% (*w*/*w*) at pH of 6.8[73,74]. Moreover, they were able to incorporate DOX in these pH-sensitive micelles by hydrophobic interactions between the drug and the hydrophobic poly (histidine) blocks when deprotonated at pH 7.4. Using MCF-7 breast cancer cells xenografts in mice, these authors observed a destabilization of the micelles and a release of DOX at the acidic pH_e that led to a significant reduction of the tumor volume and growth compared to non-pH-sensitive micelles or free DOX controls[75]. This laboratory also synthesized "flower-like" 80 nm DOX-loaded poly (L-lactic acid)-*b*-poly (ethylene glycol)-*b*-poly (L-histidine) micelles to avoid the destabilization of the micelles at acidic pH and produce a pH-induced swelling that increased the size of micelles up to 580 nm at pH 6.8 that generated the release of 60% (*w*/*w*) of DOX after 24 h (from only a 32% at pH 7.4). The authors demonstrated the pH-dependent cytotoxicity of the "flower-like" DOX-loaded micelles in MCF-7 cells, showing a reduction of cell viability from 87% at pH of 7.4−40% at pH of 6.8 and 26% at pH of 6.0, meanwhile free DOX cell viability was <20% over the entire pH range[76]. In addition, this group has described the preparation of 140 nm methoxy-poly (ethylene glycol)-*b*-(poly-L-histidine)$_2$ polymersomes with a good proton buffering capacity (between the pH values 7.4 and 5.0) and the capacity to fuse with the endolysosomal membranes of cells, which means that this system may escape from endosomes and lysosomes. At the pH range between 9.0 and 7.4 the polymersomes exhibited a stable spherical structure that was transformed to a branched and elongated structure with an equivalent hydrodynamic diameter of 400 nm at pH 6.8, which was produced by a large reduction in the hydrophobicity of poly (histidine) below the slightly acidic pH_e. This change in the structure of the polymersomes at pH 6.8 generated a very significant pH-dependent modification in the release profile of 5 (6)-carboxyfluorescein from these systems, increasing the cumulative release from 30% at pH 7.4 after 72 h to the complete release of the dye at pH 6.8 after only 4 h[77].

Johnson and coworkers[78] described the development of biocompatible hybrid polymeric vesicles based on poly (ethylene glycol) methyl ether acrylate, poly (L-lysine) and poly (L-histidine) blocks for the pH-induced intracellular delivery of DOX. As described above, poly (histidine) blocks that swell at the acidic pH_e in tumors were responsible for the structural destabilization of the vesicles, provoking a pH-induced release of the cytotoxic drug (80% at pH 5.5 after 72 h). These authors showed the pH-dependent cytotoxic response and cellular uptake of the hybrid micelles into CT26 murine cancer cells with a maximum peak at pH 5.5.

In addition of polymeric micelles, several authors have been reported the use of the poly (L-histidine) blocks to generate NPs as pH-sensitive drug delivery systems. Hwang et al.[79] described the utilization of dextran-*b*-poly (L-histidine) copolymer to manufacture DOX-loaded NPs by the nanoprecipitation dialysis method. They reported that, at the acidic tumor pH_e, the NPs swelled and released their cargo, with a pH-dependent controlled release of DOX, which doubled at acidic pH values with respect to pH 7.4. These authors showed a decrease in the viability of HuCC-T1 cholangiocarcinoma cells when incubated at the acidic tumoral pH_e with the DOX-loaded NPs, while free DOX showed an enhanced interaction and toxicity in the same cells at basic pH.

Oh's research group[80,81] described DOX-loaded self-assembled micelles based on poly (aspartic acid-*g*-imidazole)-*b*-poly (ethylene glycol) copolymer, with an isoelectric point of 6.5 and a buffering capacity between the pH values 7.5 and 5.7 as an alternative to poly (histidine) blocks. Since these micelles destabilize at pH < 7.0 and decompose at pH 6.0, these carriers showed a pH-dependent release of DOX below pH 6.5, with a cumulative release of 60% at this pH and a constant value of 37.6% within the pH range 7.0−8.0. This fact explained the absence of cytotoxicity on MCF-7 cells of the DOX-loaded micelles at that pH range and a high cytotoxicity at acidic pH (IC_{50} of 0.32 and 0.125 μg/mL at pH 6.5 and 6.0, respectively), with similar values of cell viability to those observed with the free drug. Moreover, *in vivo*, Cy5.5-labelled micelles specifically accumulated in mice bearing subcutaneous MCF-7 cells tumors, with no accumulation in the liver and the kidneys.

Ko and collaborators[82] reported DOX-loaded self-assembled methyl ether poly (ethylene glycol) (MPEG)-poly (beta-amino ester) polymeric micelles. The system showed a micellization/demicellization pH of 6.8 due to the presence of the pH-sensitive block, poly (beta-amino ester), which led to a fast release of DOX (>71% in 6 h) at pH of 6.4 with no significant release of the drug at pH 7.4 after 24 h (apart from the initial burst release of 17%). The authors showed an enhanced uptake of the DOX contained in the micelles in B16F10 melanoma cells at pH 6.4, with a cell distribution similar to the free drug. Moreover, these polymeric micelles (at 2 mg of DOX per kg) reduced the tumor volume in mice bearing subcutaneous B16F10 tumors by 72.69% from a 45.75% reduction using free DOX. In a follow-up of this work, the encapsulation of camptothecin (CPT) and tetramethylrhodamine isothiocyanate (TRITC) in the MPEG-poly (beta-amino ester) micelles for cancer theranostics purposes showed a similar micellization/demicellization at pH 6.8, producing a pH-dependent CPT cumulative release (22% at pH of 7.4 and 70% at pH of 6.4 in 24 h). The CPT-loaded micelles showed a high cytotoxicity on MDA-MB231 breast cancer cells at pH 6.4, like that produced by the free drug, but a significant lower cytotoxicity than the free drug at pH 7.4, with the carrier not contributing to the toxicity. The enhanced tumor targeting of TRITC-loaded MPEG-poly (beta-amino ester) micelles was assessed in mice bearing MDA-MB231 tumors, with an accumulation 11 times higher than that produced using TRITC-loaded non pH-sensitive micelles. Moreover, the authors described the potent antitumor capacity of CPT-loaded MPEG-poly (beta-amino ester) micelles in the same animal model with a high survival rate (67%) and almost complete inhibition of the tumor growth after 32 days at 10 mg of CPT/kg and a similar inhibition (44.8%) at a dose of 5 mg/kg within the micelles compared to the free drug at 10 mg/kg (48.6%)[83].

In an another attempt to generate pH-sensible micelles carrying a cytotoxic drug, Lee et al.[84] introduced 3-diethylaminopropyl (DEAP), as pH-sensitive moiety, and synthetized Y-shape chlorin e6 (Ce6)-loaded micelles composed of one methoxy-poly (ethylene glycol) block and two poly (L-lysine)-DEAP blocks. These micelles showed a "worm-like" structure at pH 7.4 that can be destabilized at a pH 6.8 due to the protonation of the DEAP moiety, allowing the pH-induced release of Ce6 [32% (*w*/*w*) at pH of 7.4 and 70% (*w*/*w*) at pH of 6.0 after 24 h] and an enhanced cellular uptake of the micelles in KB cells at the pH range of 6.0−6.8. Both events generated an increase in the phototoxicity of the formulation on KB cells, at pH values below 7.0 and using photosensitizing agent concentrations ranging from 0.1 to 10 μg/mL. *In vivo*, the Ce6-loaded micelles showed an enhanced tumor accumulation and a 5.2-fold tumor volume reduction compared to the free drug in nude mice bearing KB tumors.

Wang et al.[85] used methoxy poly (ethylene glycol)-*b*-poly (*N*(ε)-((1-carboxy-*cis*-cyclohexene)-2-carbonyl)-L-lysine) (mPEG-*b*-PCLL), as a pH-sensitive complex, to synthesize 89.6 nm DOX-loaded mPEG-*b*-PCLL micelles with a stable structure at pH 7.4 that swelled (up to 862 nm of hydrodynamic diameter after 24 h) and then disassembled at pH 6.8, being the process faster at pH 5.5. However, these micelles only showed a significant difference in the release profile of DOX at the intracellular pH of 5.5. Despite this, the mPEG-*b*-PCLL micelles showed an enhanced tumor growth inhibition in mice bearing H22 hepatoma cells (68.1%) compared to the free drug (47%) after 17 days, inducing larger necrotic and apoptotic areas (∼30%) and reduced toxicity.

4.1.2. *Gate opening in the nanocarriers*

The acidic pH of the tumor microenvironment can be used to induce molecular changes in the coating of porous nanocarriers that produce the opening of their pores with the consequent release of their cargo. This can be achieved through alterations in the structure/characteristics of the compounds of the NPs' coating or by the complete removal of this covering. In this section we will explain the most frequent approaches to induce a drug release process by a pH-dependent gate opening (Supporting Information Table S3).

Bilalis et al.[86] reported an innovative use for the poly (L-histidine) group as a pH-sensitive shell of the pores of mesoporous silica NPs, being "nanogates" that are opened with the slightly acidic pH_e in tumors. They loaded DOX inside the nano-channels of the NPs that was released in a controlled way only under acidic pH, with a significantly enhanced release at the highly acidic conditions (pH = 5.0) in the intracellular organelles after endocytic uptake. Chen et al.[87] coated DOX-loaded PEGylated silica NPs with the pH-sensitive "gatekeeper" poly (2-pentamethylenimino) ethyl methacrylate (PPEMA) to close the pores of the NPs at physiological pH, avoiding the release of DOX during blood circulation (cumulative release of less than 15% at pH 7.4). At pH 6.5 the pores opened, releasing the cytotoxic drug (68%) due to the protonation of PPEMA that reversed the charge of the NPs from negative (−22.6 mV) to positive (+69.4 mV), which facilitated cellular DOX uptake. These NPs exhibited an IC_{50} value on HeLa cells of 21.75 μg/mL. Recently, Chen et al.[88] described the coating of DOX-loaded silica NPs with chitosan crosslinked with *N*,*N*′-bis(acryloyl)cystamine (BAC) by disulfide bonds to protect the cytotoxic drug during blood circulation (cumulative release of 10.4% at pH 7.4) and induce their release at

pH 6.5 (29.7%), with the addition of 10 mmol/L glutathione (GSH) (highly expressed in cancer) (42.9%), or by the combined action of both factors (48.6%). This pH/GSH-dependent release of DOX is due to the protonation of the crosslinked chitosan at the pH_e that is removed from the NPs surface and the breakage of the disulfide bonds of BAC by the action of glutathione. The system showed similar cytotoxicity values in HepG-2 cells compared to free DOX, being increased when the folate ligand was included in the surface of the NPs due to a receptor-mediated endocytosis.

4.1.3. *Acid-labile linkers*

Cytotoxic drugs, in addition to their encapsulation in pH-sensitive nanocarriers, can be conjugated in the surface of the carrier using acid-labile linkers, such as phosphoramidate, imine, orthoester or hydrazone. However, most of the articles found in the literature about drug-conjugated carriers are focused on intracellular pH-dependent drug delivery at pH values ranged between 5.0 and 6.0 and, with the exception of the 2,3-dimethylmaleic anhydride (DMMA) linker[89–93] (Supporting Information Table S4), these pH-sensitive linkers are almost unresponsive to the slightly acidic extracellular tumoral pH. In fact, Liu et al.[94] reported a dual delivery system for breast cancer treatment by immunotherapy and chemotherapy, where they combined the pH-sensitive poly (histidine) block and the acid-labile hydrazone linker. These authors generated NPs by the nanoprecipitation method, using poly (histidine) and the R848 immune modifier. NPs were subsequently coated with a conjugate of DOX and hyaluronic acid (HA), using the hydrazone linker. At the tumor pH_e, poly (histidine) chains protonated, provoking the release of the R848 to regulate the immune response. Once the NPs were uptake by CD44-mediated endocytosis, using the HA as active targeting ligand, the hydrazone linker was cleavage at pH 5.5, releasing the cytotoxic drug (DOX) in the intracellular region and reducing cell viability of breast cancer cells. This dual system showed tumor growth inhibition in 4T1 tumor-bearing mice.

To achieve a regulated release of DOX, Wu et al.[95] incorporated DMMA to poly (D,L-lactide)-*b*-poly (2-aminoethyl methacrylate) (PLA-*b*-PAEMA) to obtain PLA-*b*-PAEMA/DMMA block copolymers and then self-assembled NPs with a core of PLA and a shell of PAEMA/DMMA with charge modification properties by the hydrolysis of DMMA at pH_e (the NPs have a negative charge at pH 7.4 but positive at pH 6.5). Positively charge DOX·HCl were included into the negatively charged NPs (−18.3 mV) at physiological pH due to electrostatic interactions (with a small cumulative release of around 20%) and released at pH of 6.5 (cumulative release of 75%) because of the hydrolysis of DMMA, which confers a positive charge to the NPs (+4.4 mV) breaking the electrostatic interactions between the drug and the carrier. In HeLa cells, the DOX-loaded PLA-*b*-PAEMA/DMMA NPs demonstrated an enhanced intracellular distribution and the nanocarrier showed a potent cytotoxicity at pH 6.5 (75% of viable cells at a nanocarrier concentration of 6.25 μg/mL and 15% at 100 μg/mL). Using a similar strategy, Feng et al.[96] described the complexation of the positively charged cisplatin (IV) prodrug-conjugated carbon dots with the negatively charged poly (ethylene glycol)-poly (allyamine hydrochloride)/DMMA (PEG-(PAH/DMMA) by electrostatic interactions. When the pH was reduced to 6.8, the hydrolysis of DMMA modified the charge of PEG-(PAH/DMMA) from negative to positive, which led to the removal of this polymer from the surface of the cisplatin (IV) produg-conjugated carbon dots. In A2780 cancer cells, this system showed at pH 6.8 an enhanced cellular uptake because of their positive charge after the hydrolysis of DMMA and a potent cytotoxicity due to the release of the prodrug (cumulative release of more than 70% at pH 6.8 and 10 mmol/L of GSH) that was reduced to cisplatin. *In vivo* at a dose of 1.5 mg of platinum per kg of body weight a 9-fold tumor growth inhibition was achieved compared to controls, after 14 days of treatment in mice bearing subcutaneous cervix U14 xenografts, with no signs of toxicity to the animals.

4.2. *Favoring the pH-dependent internalization of nanocarriers*

In addition to their use for the pH-dependent release of cytotoxic drugs, pH-sensitive blocks have been also used to promote the internalization of nanocarriers by either mediating pH-induced modifications to the charge on the nanocarrier surface, or stimulating the active targeting function in the nanocarrier or removing the PEG chains when exposed to the pH_e in tumors.

4.2.1. *pH-induced surface charge modification*

One of the approaches most frequently employed to enhance the internalization of the nanocarriers is to use the acidic tumoral environment to induce a change in the charge of these nanocarriers (Supporting Information Table S5). At a physiological pH the nanocarriers show a negatively charged surface, but protonation upon environment acidification near the tumors leads to a reversion in the charge that allows the internalization of the nanocarriers by the cancer cells.

Hu et al.[97] combined a positively charged paclitaxel-loaded poly (L-histidine)/polyethyleneimine-based micelles with the pH-sensitive negatively charged block α-methoxy ω-hydroxy poly (ethylene glycol)-*b*-polysulfadimethoxine (mPEG-*b*-PSDM) by electrostatic complexation to enhance their stability in blood at physiological pH. The protonation at pH 6.9 of the negatively charged PSDM, a sulfonamide derivative, led to the dissociation of mPEG-*b*-PSDM from the positively charged micelles, being the charge reversal from negative to positive completed at pH 6.6. As mentioned above (section 4.1.A), the inclusion of the poly (histidine) group in the micelles generated the pH-dependent release of paclitaxel (cumulative release of 10% at pH 7.4 and 70% at pH 6.6). The system showed an enhanced cellular uptake at pH 6.6 in MCF-7 and SKOV-3 cancer cells compared to the minimal non-specific uptake at pH of 7.4. Moreover, the authors demonstrated the potent cytotoxicity of the paclitaxel-loaded micelles in MCF-7 cells, with similar values of IC_{50} (37 ng/mL) than the free drug (24 ng/mL) at pH 6.6 and a reduced cytotoxicity at pH 7.4 (IC_{50} of 295 ng/mL). *In vivo*, this formulation exhibited a deep tumor penetration and a 2.2-fold tumor growth inhibition compared to the treatment with the free drug after 29 days in a mice MCF-7 model[97].

Ye et al.[98] synthetized smart hybrid DOX-loaded NPs by the nanoprecipitation method. These NPs were composed of a PEGylated lipid shell, which provides the biocompatible and stealth character to the NPs, and a poly (histidine) core to facilitate both intracellular uptake and controlled drug release inside the cells after internalization in a pH-dependent two-phase process. A) A first phase at the pH_e in tumors (6.5−7.0) with the movement of the poly (histidine) blocks to the surface due to the swelling of the NPs at this pH, which produces a partial release of the drug and a shift in the surface charge from negative to neutral or slightly positive that facilitates the intracellular uptake of the NPs. B) Once the NPs were internalized, in a second phase, there is a complete destabilization of the NPs at values of pH between 4.5

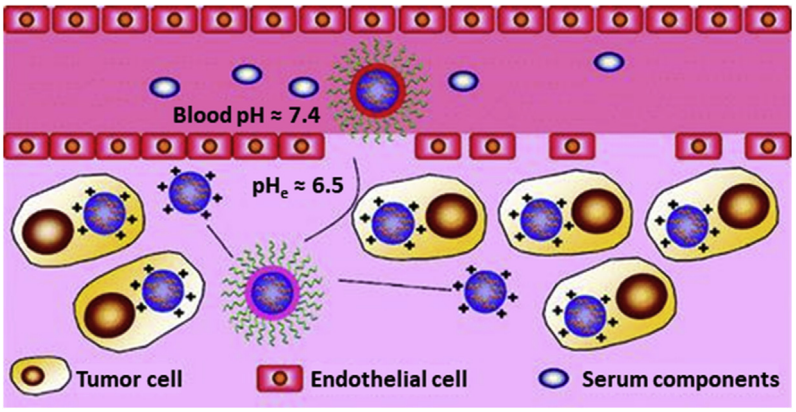

Figure 8 Scheme of siRNA-loaded PEGylated NPs that shows reduced non-specific interactions with blood proteins at physiological pH. However, at the slightly acidic pH_e, PEG molecules are removed from the surface of the NPs because of their acid-cleavable DMMA linker, promoting the intracellular delivery of the siRNA. Reprinted with permission from Ref. 106. Copyright © 2012 American Chemical Society.

and 6.5, producing the total release of the cargo of the NPs in the cytoplasm. *In vivo*, this drug delivery system increased the antitumor efficacy of free DOX in 4T1 tumor-bearing mice.

Du and co-workers[99] modified poly (2-aminoethyl methacrylate hydrochloride) (PAMA) nanogels with DMMA to obtain DOX-loaded carriers with a pH-induced tunable surface charge from negative at physiological pH to positive at the slightly acidic pH_e in tumors (pH = 6.8). The PAMA-DMMA nanogels possessed a negative charge during their circulation in blood, which avoids the interaction with the blood proteins, and a positive charge once in the tumor microenvironment at pH 6.8, which promotes their efficient intracellular uptake. Positively charged DOX was efficiently loaded to the negatively charged nanogels by electrostatic interactions at physiological pH and completely released at the acidic pH of the intracellular organelles (pH = 5.5) by electrostatic repulsion because of the positive charge of the nanogels from the pH_e. The authors showed a higher decrease in cell viability in MDA-MB-435s cells when cultured with this formulation with respect to PAMA nanogels without the acid-labile DMMA. The administration of the PAMA-DMMA and PAMA nanogels in MDA-MB-435s tumor-bearing mice showed an intracellular location of the former and an extracellular distribution of the latter, which confirmed *in vitro* results and demonstrated the enhanced intracellular uptake of the PAMA-DMMA nanogels at the tumor pH_e. Using a similar strategy, Yoon et al.[100] modified a DOX-loaded octadecyl grafted poly (2-hydroxyethyl aspartamide) micelles with the DMMA block to include charge reversal properties (from −14.3 mV at pH 7.4 to +10.0 mV at pH 6.8), which are produced by the detachment of DMMA from the nanocarrier at the pH_e. These DOX-loaded micelles showed a pH-dependent cellular uptake and an enhanced cytotoxicity in MB-435 cancer cells compared to free DOX after 3 h of treatment. Huang et al.[101] used the pH-sensitive citraconic anhydride, a derivative of DMMA, to synthesize poly (aspartate)-*g*-poly (ethylene glycol)-dodecylamine-(hydrazone-doxurubicin)-(ethylene-diamine-citraconic amide) conjugates and obtain 60 nm DOX-loaded micelles. The formation of citraconic amides in the conjugates led to a charge modification in the surface of the micelles at pH 6.6 when these bonds were cleaved. Altering the zeta potential of the micelles, from −20 mV at pH 7.4 to +15 mV at pH 6.6, significantly improved their cellular uptake at pH_e by HepG2 cells after 24 h, compared to the values obtained at pH 7.4. Once internalized, the micelles showed an increased release of DOX at pH 5.0 because of the breakage of the hydrazone bond. The DOX-loaded micelles showed a potent cytotoxicity in HepG2 cells (20% of viable cells after 24 h at 5 μg/mL DOX), with similar values compared to free DOX at the same concentration. Recently, Qu et al.[102] have reported DOX-loaded poly (lysine-*co*-*N*,*N*-bis(acryloyl) cystamine-*co*-dimethylmaleic anhydride (PLB-DMMA) negatively charged hybrid micelles that change to positive at pH_e upon DMMA cleavage, facilitating this reversion their cellular uptake by HeLa cells. The internalized micelles can be then disassembled by swelling at pH 5.0 and degradation of the disulfide bonds in the polymer chain with redox agents (10 mmol/L GSH), resulting in a DOX release of 86% and a significant cytotoxicity in HeLa cells after 24 h (IC_{50} of 61.7 μg/mL at pH 6.5).

4.2.2. *pH-Induced activation of ligands*

This approach uses pH sensitive structures to protect the active targeting moieties of the nanocarriers during blood circulation until they reach the acid tumoral microenvironment that activates the ligands to promote the internalization of the nanocarriers (Supporting Information Table S6).

Quan et al.[103] described the synthesis of DOX-loaded PEGylated micelles, based on an α-β cyclodextrin dimer and a modified *N*-isopropylacrylamide-*co*-*N*-acroyloxysuccinimide (P(NIPAAm-*co*-NAS), that included a RGD peptide (Arg-Gly-Asp) as the targeting ligand to enhance the cellular uptake of the nanocarrier. In the micelles the RGD peptide was protected by PEG chains at physiological pH during blood circulation, but the ligand was exposed at pH below 6.8 due to the PEG removal after the hydrolysis of the benzoic-imine bonds that were used for PEGylation, enhancing the cellular uptake of micelles by endocytosis at pH_e in HeLa cells. Moreover, the detachment of PEG molecules from the micelles changed their critical solution temperature from 38 °C at pH 7.4−35.5 °C at pH_e, which generated a temperature-induced release of DOX since micelles were stable at physiological conditions but their structure was disassembled at pH below 6.8. The authors observed a significant decrease (74%) in cell viability of HeLa cells when incubated with the DOX-loaded micelles at pH 6.8 and temperatures above 37 °C.

Using a completely different approach, Zhang et al.[104] prepared silica NPs loaded with DOX and functionalized with β-

cyclodextrin (β-CD) *via* disulfide bond and then with two peptide sequences, Arg-Gly-Asp (RGD) and Pro-Leu-Gly-Val-Arg (PLGVR) *via* host-guest complexation. To protect the targeting moiety (RGD), poly (aspartic acid) (PASP) was included *via* click chemistry to PLGVR. During blood circulation, the silica NPs were shielded from non-specific cellular uptake, but at pH_e they were internalized by SCC-7 and HT-29 cancer cells. At this pH_e the PLGVR is hydrolyzed by the action of matrix metalloproteinases (MMPs), which leads to the exposure of the RGD moiety (53.6% of PASP was detached from NPs after 4 h with MMP-2) and uptake of the NPs. Once internalized, the DOX loaded in the pores of the silica NPs can be released by the cleavage of the disulfide bond with the action of GSH that removes the β-CD that close the pores (70% of DOX was released with 10 mmol/L GSH in 1 h, while no release was produced in the absence of GSH). Moreover, the authors demonstrated that these NPs have a potent cytotoxic effect on SCC-7 and HT-29 cells, since only the 40%−50% of cells remain viable after their treatment with the DOX-loaded silica NPs at a dose of DOX of 2.5 μg/mL.

Recently, Pan et al.[105] synthetized by the nanoprecipitation method smart NPs composed of a D-α-tocopheryl polyethylene glycol succinate-poly (histidine)-folate (TPGS-Phis-folate) triblock copolymer plus a methoxypoly (ethylene glycol)-poly (D,L-lactic acid) (mPEG-PLA) diblock copolymer. PEG was included on the surface of the NPs to increase the blood circulation lifetime of the NPs, while the poly (histidine) block was added for the pH-dependent release of the cytotoxic drug and the pH-dependent activation of folate, the active targeting moiety that is hidden under the PEG layer at the physiological pH. When poly (histidine) is protonated at the pH_e in tumors, the swelling of the NPs moves the targeting moiety to the surface of the NPs, facilitating their internalization into 4T1 breast cancer cells. After NPs endocytosis, the poly (histidine) residues promoted the complete dissociation of the NPs at the acidic pH of the intracellular organelles, and therefore the release of the cytotoxic drug, docetaxel, into the cytoplasm of the cells. These pH-sensible docetaxel-loaded NPs showed a pH-dependent cytotoxicity profile, with a 1.66- and 3.83-fold decrease in the cell viability at pH of 6.8 and 5.8, respectively, which pointed to a partial release of docetaxel in the tumor microenvironment and the total release in the intracellular space.

4.2.3. *pH-Induced PEG detachment*

Another strategy to induce the uptake of the nanocarriers using the acidic pH of the tumor environment is to link the PEG chains by pH-sensitive structures (Supporting Information Table S7). The PEG will protect the nanocarriers in circulation, but this stabilization layer will be detached when exposed to the slightly acidic pH of the tumors to avoid the hindering of the internalization of the carriers by the cancer cells due to PEGylation.

In addition to its role in modifying the surface charge of the nanocarriers from negative to positive, DMMA is also used to remove the stealth PEG layer of nanocarriers once in the extracellular tumor microenvironment and thus, increase their cellular uptake.

Yang et al.[106] coated thiolated polyethyleneimine/siRNA NPs with the pH-sensitive PPC-DMMA, which is composed of the PEGylated poly (2-(2-aminoethoxy)ethoxy)phosphazene (mPEG-PAEP) diblock copolymer, cysteamine and DMMA. This formulation was used for the delivery of Polo like kinase 1 (Plk1) siRNA into MDA-MB-231 cells and MDA-MB-231 xenografts. At physiological pH, the NPs showed a reduction in the nonspecific interactions with blood proteins because of the PEG chains, facilitating their blood circulation, while at the tumor pH_e the PEG molecules detached and the siRNA-loaded NPs displayed a positive charge at their surface, promoting the intracellular uptake of siRNA and increasing the efficiency of gene silencing in MDA-MB-231 cells and mice with MDA-MB-231 xenografts, where the formulation reduced tumor growth, decreasing proliferation and increasing cell death (Fig. 8).

Using a similar approach, Fan et al.[107] described positively charged microRNA (miR-34a)-loaded NPs based on β-cyclodextrin and polyethylenimine (PEI). As Yang and co-workers[106], they coated these NPs with a negatively charged PEG derivative modified with DMMA (PPC-DMMA) that include pH-sensitive characteristics. The DMMA-modified PEGylated shell of the NPs protects them from the non-specific adsorption of proteins at physiologic pH during blood circulation (24 h) and can be removed at pH_e, enhancing their cellular uptake, by the cleavage of the amide bonds in the PPC-DMMA block copolymer, which generates a charge reversal from negative to positive. The authors showed the enhanced cellular uptake of the NPs at pH 6.8 in CD44-expressing B16F10 melanoma cells compared to the values obtained at pH 7.4, increasing the intracellular release of miR-34a and, therefore, reducing the CD44 expression. *In vivo*, using mice bearing B16F10 xenografts, the complexes accumulated in the tumors and exhibited a 1.6-fold tumor growth inhibition compared to free miR-34a.

4.3. *pH-Sensitive size reduction for tumor penetration of nanocarriers*

Another problem to deliver cytotoxic drugs to cancerous cells is their ability to overcome the poor vasculature and dense extracellular matrix in tumors to reach the inside of the tumoral mass. Nanocarriers can be engineered to change their size as a function of the acidic pH of the tumor microenvironment. At physiological pH, particle size is larger in order to possess optimal pharmacokinetic and pharmacodynamic properties, but, at pH_e, the particles decrease in size below 30 nm to circumvent the biological barriers and penetrate in the tumoral mass.

Li et al.[108] synthetized a platinum prodrug-conjugated poly (ethylene glycol)-*b*-poly (2-azepane ethyl methacrylate)-modified polyamido-amine (PEG-*b*-PAEMA-PAMAM/Pt) dendrimers with an enhanced tumor penetration capacity in the pH_e range because of the pH-sensitive PAEMA block. This structure is self-assembled at pH 7.4 with a diameter of 80 nm, but is rapidly dissociated into its building blocks (10 nm of size) at pH 6.7, which led to a deep tumor penetration (85 μm) and up to 2.9-fold enhanced cell internalization of Cy5-labeled PEG-*b*-PAEMA-PAMAM dendrimers in pancreatic BxPC-3 multicellular spheroids at this pH_e, compared to the free Cy5 or Cy5-labeled pH-insensitive dendrimers that were only located at the surface of the spheroids. Moreover, the PEG-*b*-PAEMA-PAMAM/Pt dendrimers exhibited a 2-fold increase in cell apoptosis (45%) at pH 6.7 in the spheroids, compared to the values obtained for Pt-conjugated pH-insensitive dendrimers or the PEG-*b*-PAEMA-PAMAM/Pt dendrimers at physiological pH. *In vivo*, these dendrimers showed a long circulation time in blood of more than 7 h in mice and a strongly inhibited tumor growth (up to 82% at a dose of 2 mg/kg) in mice bearing a pancreatic BxPC-3 xenograft compared to free cisplatin (24% at a dose of 2 mg/kg).

In another report this research group reported platinum prodrug-loaded clustered nanoparticles based on poly (amido-amine)-(2-propionic-3-methylmaleic anhydride)-polycaprolactone (PAMAM-CDM-PCL), PCL homopolymer and poly (ethylene glycol)-*b*-poly (*ε*-caprolactone) (PEG-*b*-PCL) copolymer. This system showed 100 nm of size and high stability at physiological pH during blood circulation (half-time higher than 10 h) due to the PEG-*b*-PCL layer but, at the pH_e and because of PCL, was dissembled in 5 nm platinum prodrug-functionalized PAMAM dendrimers with a 10-fold enhanced penetration in BxPC-3 pancreatic cancer cells spheroids compared to non-pH sensitive clustered nanoparticles. Once internalized, the dendrimers were reduced, releasing the cytotoxic cisplatin. The pH-sensitive clustered nanoparticles exhibited significant tumor inhibitions of 88% or 95% in mice bearing BxPC-3 tumors or cisplatin-resistant A549R lung tumors compared to free cisplatin (38% or 10%) or non-sensitive clustered nanoparticles (57% or 60%)[109].

5. Conclusions and future perspectives

Many works have been published in the last decade regarding the use of nanocarriers as an effective approach to specifically deliver anticancer drugs to tumors[19]. The success of this approach for targeted and/or safe delivery of chemotherapeutic drugs is stressed by the fact that some liposomal or PEGylated formulations are already being used in hospitals worldwide, but in addition, many clinical trials are being carried using encapsulated cytotoxic drugs[110].

Targeted delivery can only be achieved when the nanocarriers are able to distinguish between normal and tumoral tissues, and the differences in intra- and extracellular pH is a common characteristic of solid tumors of which researchers can take advantage to design delivery systems. Thus, almost a thousand articles come up when searching for nanocarriers and pH only in the title in PubMed, which is a testimony to the relevance of this approach as a therapeutic option.

In this monograph we have included some examples that illustrate the vast application of the drug delivery systems to the pH-based paradigm in cancer, focusing on a) the generation of acid stress inside the cancerous cells by proton-caged carriers, b) the inhibition of the proton extruder systems to promote acid-induced apoptosis in cancerous cells as well as to increase the acidic pH_e and avoid the MDR by different nano-scale platforms, normally used as adjuvant therapy to cytotoxic drugs, and c) the utilization of the anomalous slightly acidic extracellular milieu in cancer to generate a controlled intracellular drug delivery.

Despite the vast amount of work done on proton pumps and their role in the pH changes observed in the tumoral extracellular environment and in cancer progression, there are no inhibitors approved for their use in cancer treatment. Moreover, among the transporters mentioned in this review, only carbonic anhydrase inhibitors are being tested in clinical trials as potential anticancer drugs. As we have mentioned before, vacuolar ATPases and Na^+/H^+ exchangers are overexpressed in several types of cancer (Tables 2 and 3) and are likely responsible, at least in part of the extracellular acidification observed in cancer. This stresses the need of further research on these families in order to find and test new inhibitors capable of blocking cancer growth and dissemination.

Most of the approaches to use the extracellular acidic pH of tumors for a targeted delivery of cytotoxic drugs have shown a higher efficiency of the drug-loaded pH sensible carriers than the administration of the free drugs, validating the use of extracellular pH changes to target tumors and avoid toxicity. But in spite of the success in treating cells in culture or mouse cancer models, these pH-based strategies for drug delivery have only reached preclinical stages, and to the best of our knowledge, to date no clinical trials involving pH sensitive drug delivery systems have been performed. This important step is a common barrier where most new drugs or therapeutic strategies end their development. Thus, unexpected toxicity not observed in mice, ineffectiveness in human beings or inability to scale up the synthesis of the compounds are some of the most frequent insurmountable barriers that researchers find that block the advance to clinical trials. This is a young area of interest in cancer therapeutics and future work is needed to optimize this therapeutic option and make it useful for cancer treatment.

The anomalous metabolism of cancer cells opens up a large number of new opportunities and strategies to fight against cancer as a unique illness. Although some of these approaches were not included in this monography because they are less explored in association with drug delivery systems, we would like to, at least, mention them as future perspectives in this promising field. The induction of lysosomal membrane permeabilization (LMP), which has usually been achieved by the utilization of lysomotropic detergents, is one of the strategies to produce intracellular acidification and induce apoptosis, but it entails numerous side effects due to its lack of specificity. Although superparamagnetic iron oxide NPs (SPIONs) have been used for the generation of hyperthermia and magnetic-induced controlled drug release, they have not been widely explored for LMP, being this approach of great interest. In fact, epidermal growth factor (EGF)- or lysosomal protein marker LAMP1-conjugated SPIONs can be targeted to lysosomes and exposed to low frequency alternating magnetic fields (AMF) to generate rotation of the NPs inside the organelles that destabilize their membranes producing important mechanical damage[111–114]. A recent approach to revert the abnormal metabolic behavior in cancer cells is the inhibition of the shift of the oxidative phosphorylation to the aerobic glycolysis by the delivery to the mitochondria of dichloroacetate (DCA), an inhibitor of the pyruvate dehydrogenase kinase (PDK). The numerous problems regarding to the bioavailability, stability and intracellular uptake to the mitochondria of this compound can be resolved by the vehiculization of DCA by backbone carriers conjugated to DCA, pro-haloacetate NPs or nanomicelles generated from polymer–DCA conjugates that successfully target the mitochondria of cancer cells and interact with the PDK protein, increasing the oxidative phosphorylation process and inducing apoptosis of the malignant cells[115–118]. Although, the acidic tumoral pH_e has been typically used to generate a pH-induced focalized and controlled drug release by pH-sensitive carriers, some research is currently underway to reverse this anomalous pH by using aqueous-stable calcium carbonate NPs with buffering capacity in order to minimize the MDR[119,120]. Despite the present lack of drugs or nanocarriers using extracellular acidification as a therapeutic approach in the clinical practice, this pH reduction in the tumor microenvironment is a common characteristic of solid tumors, and, thus,

offers a unique weakness that can't be overviewed in the global race to find a cure for cancer.

Author contributions

Dr. Pérez-Herrero and Dr. Fernández-Medarde wrote and revised the manuscript. All authors have read and approved the final text and consent to its publication.

Conflicts of interest

These authors have no conflicts of interest to declare in this work.

Appendix A. Supporting Information

Supporting data to this article can be found online at https://doi.org/10.1016/j.apsb.2021.01.012.

References

1. Anandakrishnan R, Varghese RT, Kinney NA, Garner HR. Estimating the number of genetic mutations (hits) required for carcinogenesis based on the distribution of somatic mutations. *PLoS Comput Biol* 2019;**15**:e1006881.
2. Iranzo J, Martincorena I, Koonin EV. Cancer-mutation network and the number and specificity of driver mutations. *Proc Natl Acad Sci U S A* 2018;**115**:E6010.
3. Harguindey S, Reshkin SJ. "The new pH-centric anticancer paradigm in Oncology and Medicine"; SCB, 2017. *Semin Cancer Biol* 2017;**43**:1−4.
4. Hanahan D, Weinberg RA. Hallmarks of cancer: the next generation. *Cell* 2011;**144**:646−74.
5. Bellou S, Pentheroudakis G, Murphy C, Fotsis T. Anti-angiogenesis in cancer therapy: hercules and hydra. *Cancer Lett* 2013;**338**:219−28.
6. Huang M, Deng J, Gao L, Zhou J. Innovative strategies to advance CAR T cell therapy for solid tumors. *Am J Cancer Res* 2020;**10**:1979−92.
7. Dumas JF, Brisson L, Chevalier S, Mahéo K, Fromont G, Moussata D, et al. Metabolic reprogramming in cancer cells, consequences on pH and tumour progression: integrated therapeutic perspectives with dietary lipids as adjuvant to anticancer treatment. *Semin Cancer Biol* 2017;**43**:90−110.
8. Harguindey S, Stanciu D, Devesa J, Alfarouk K, Cardone RA, Polo Orozco JD, et al. Cellular acidification as a new approach to cancer treatment and to the understanding and therapeutics of neurodegenerative diseases. *Semin Cancer Biol* 2017;**43**:157−79.
9. Marbaniang C, Kma L. Dysregulation of glucose metabolism by oncogenes and tumor suppressors in cancer cells. *Asian Pac J Cancer Prev APJCP* 2018;**19**:2377−90.
10. Yeung SJ, Pan J, Lee MH. Roles of p53, MYC and HIF-1 in regulating glycolysis—the seventh hallmark of cancer. *Cell Mol Life Sci* 2008;**65**:3981−99.
11. Koltai T. Triple-edged therapy targeting intracellular alkalosis and extracellular acidosis in cancer. *Semin Cancer Biol* 2017;**43**:139−46.
12. Stock C, Pedersen SF. Roles of pH and the Na^+/H^+ exchanger NHE1 in cancer: from cell biology and animal models to an emerging translational perspective?. *Semin Cancer Biol* 2017;**43**:5−16.
13. Huber V, Camisaschi C, Berzi A, Ferro S, Lugini L, Triulzi T, et al. Cancer acidity: an ultimate frontier of tumor immune escape and a novel target of immunomodulation. *Semin Cancer Biol* 2017;**43**:74−89.
14. Omran Z, Scaife P, Stewart S, Rauch C. Physical and biological characteristics of multi drug resistance (MDR): an integral approach considering pH and drug resistance in cancer. *Semin Cancer Biol* 2017;**43**:42−8.
15. Gdovin MJ, Kadri N, Rios L, Holliday S, Jordan Z. Focal photodynamic intracellular acidification as a cancer therapeutic. *Semin Cancer Biol* 2017;**43**:147−56.
16. Du JZ, Li HJ, Wang J. Tumor-acidity-cleavable maleic acid amide (TACMAA): a powerful tool for designing smart nanoparticles to overcome delivery barriers in cancer nanomedicine. *Acc Chem Res* 2018;**51**:2848−56.
17. Taylor S, Spugnini EP, Assaraf YG, Azzarito T, Rauch C, Fais S. Microenvironment acidity as a major determinant of tumor chemoresistance: proton pump inhibitors (PPIs) as a novel therapeutic approach. *Drug Resist Updates* 2015;**23**:69−78.
18. Kolosenko I, Avnet S, Baldini N, Viklund J, De Milito A. Therapeutic implications of tumor interstitial acidification. *Semin Cancer Biol* 2017;**43**:119−33.
19. Perez-Herrero E, Fernandez-Medarde A. Advanced targeted therapies in cancer: drug nanocarriers, the future of chemotherapy. *Eur J Pharm Biopharm* 2015;**93**:52−79.
20. Neri D, Supuran CT. Interfering with pH regulation in tumours as a therapeutic strategy. *Nat Rev Drug Discov* 2011;**10**:767.
21. Asgharzadeh MR, Barar J, Pourseif MM, Eskandani M, Jafari Niva M, Mashavekhi MR, et al. Molecular machineries of pH dysregulation in tumor microenvironment: potential targets for cancer therapy. *Bioimpacts* 2017;**7**:115−33.
22. Parks SK, Pouysségur J. Targeting pH regulating proteins for cancer therapy—progress and limitations. *Semin Cancer Biol* 2017;**43**:66−73.
23. Spugnini E, Fais S. Proton pump inhibition and cancer therapeutics: a specific tumor targeting or it is a phenomenon secondary to a systemic buffering?. *Semin Cancer Biol* 2017;**43**:111−8.
24. Collins MP, Forgac M. Regulation and function of V-ATPases in physiology and disease. *Biochim Biophys Acta Biomembr* 2020;**1862**:183341.
25. Jefferies KC, Cipriano DJ, Forgac M. Function, structure and regulation of the vacuolar (H^+)-ATPases. *Arch Biochem Biophys* 2008;**476**:33−42.
26. Izumi H, Torigoe T, Ishiguchi H, Uramoto H, Yoshida Y, Tanabe M, et al. Cellular pH regulators: potentially promising molecular targets for cancer chemotherapy. *Cancer Treat Rev* 2003;**29**:541−9.
27. Stransky L, Cotter K, Forgac M. The function of V-ATPases in cancer. *Physiol Rev* 2016;**96**:1071−91.
28. Federici C, Lugini L, Marino ML, Carta F, Lessi E, Azzarito T, et al. Lansoprazole and carbonic anhydrase IX inhibitors sinergize against human melanoma cells. *J Enzym Inhib Med Chem* 2016;**31**:119−25.
29. Alai MS, Lin WJ. A novel nanoparticulate system for sustained delivery of acid-labile lansoprazole. *Colloids Surf B Biointerfaces* 2013;**111**:453−9.
30. Alai M, Lin WJ. Novel lansoprazole-loaded nanoparticles for the treatment of gastric acid secretion-related ulcers: *in vitro* and *in vivo* pharmacokinetic pharmacodynamic evaluation. *AAPS J* 2014;**16**:361−72.
31. Alai M, Lin WJ. Application of nanoparticles for oral delivery of acid-labile lansoprazole in the treatment of gastric ulcer: *in vitro* and *in vivo* evaluations. *Int J Nanomed* 2015;**10**:4029−41.
32. Granja S, Tavares-Valente D, Queirós O, Baltazar F. Value of pH regulators in the diagnosis, prognosis and treatment of cancer. *Semin Cancer Biol* 2017;**43**:17−34.
33. Paškevičiūtė M, Petrikaitė V. Proton pump inhibitors modulate transport of doxorubicin and its liposomal form into 2D and 3D breast cancer cell cultures. *Cancer Manag Res* 2019;**11**:9761−9.
34. Lugini L, Federici C, Borghi M, Azzarito T, Marino ML, Cesolini A, et al. Proton pump inhibitors while belonging to the same family of generic drugs show different anti-tumor effect. *J Enzym Inhib Med Chem* 2016;**31**:538−45.
35. Azzarito T, Venturi G, Cesolini A, Fais S. Lansoprazole induces sensitivity to suboptimal doses of paclitaxel in human melanoma. *Cancer Lett* 2015;**356**:697−703.

36. Yu M, Lee C, Wang M, Tannock IF. Influence of the proton pump inhibitor lansoprazole on distribution and activity of doxorubicin in solid tumors. *Cancer Sci* 2015;**106**:1438−47.
37. Bhattacharya S, Khanam J, Sarkar P, Pal TK. A chemotherapeutic approach targeting the acidic tumor microenvironment: combination of a proton pump inhibitor and paclitaxel for statistically optimized nanotherapeutics. *RSC Adv* 2019;**9**:240−54.
38. Loo SY, Chang MK, Chua CS, Kumar AP, Pervaiz S, Clement MV. NHE-1: a promising target for novel anti-cancer therapeutics. *Curr Pharmaceut Des* 2012;**18**:1372−82.
39. Amith SR, Fliegel L. Na^+/H^+ exchanger-mediated hydrogen ion extrusion as a carcinogenic signal in triple-negative breast cancer etiopathogenesis and prospects for its inhibition in therapeutics. *Semin Cancer Biol* 2017;**43**:35−41.
40. Chen Q, Liu Y, Zhu Xl, Feng F, Yang H, Xu W. Increased NHE1 expression is targeted by specific inhibitor cariporide to sensitize resistant breast cancer cells to doxorubicin *in vitro* and *in vivo*. *BMC Cancer* 2019;**19**:211.
41. Tate JG, Bamford S, Jubb HC, Sondka Z, Beare DM, Bindal N, et al. COSMIC: the catalogue of somatic mutations in cancer. *Nucleic Acids Res* 2019;**47**(D1):D941−7.
42. Zheng T, Jäättelä M, Liu B. pH gradient reversal fuels cancer progression. *Int J Biochem Cell Biol* 2020;**125**:105796.
43. Perez-Escuredo J, Van Hee VF, Sboarina M, Falces J, Payaen VL, Pellerin L, et al. Monocarboxylate transporters in the brain and in cancer. *Biochim Biophys Acta* 2016;**10**:16.
44. Calori IR, Piva HL, Tedesco AC. Targeted cancer therapy using alpha-cyano-4-hydroxycinnamic acid as a novel vector molecule: a proof-of-concept study. *J Drug Deliv Sci Technol* 2020;**57**:101633.
45. Guan X, Morris ME. *In vitro* and *in vivo* efficacy of AZD3965 and alpha-cyano-4-hydroxycinnamic acid in the murine 4T1 breast tumor model. *AAPS J* 2020;**22**:84.
46. Payen VL, Mina E, Van Hée VF, Porporato PE, Sonveaux P. Monocarboxylate transporters in cancer. *Mol Metab* 2020;**33**:48−66.
47. Clinical trials. Available from: https://www.clinicaltrials.gov. [Accessed 3 October 2020].
48. Huang T, Feng Q, Wang Z, Li W, Sun Z, Wilhelm J, et al. Tumor-targeted inhibition of monocarboxylate transporter 1 improves T-cell immunotherapy of solid tumors. *Adv Healthc Mater* 2020;**10**:2000549.
49. Mboge MY, Mahon BP, McKenna R, Frost SC. Carbonic anhydrases: role in pH control and cancer. *Metabolites* 2018;**8**:19.
50. GEO profile dataset. Available from: https://www.ncbi.nlm.nih.gov/geoprofiles. [Accessed 10 October 2020].
51. Oosterwijk E. Carbonic anhydrase expression in kidney and renal cancer: implications for diagnosis and treatment. In: Frost SC, McKenna R, editors. *Carbonic anhydrase: mechanism, regulation, links to disease, and industrial applications*. Dordrecht: Springer Netherlands; 2014.
52. Tatiparti K, Rauf MA, Sau S, Iyer AK. Carbonic anhydrase-IX guided albumin nanoparticles for hypoxia-mediated triple-negative breast cancer cell killing and imaging of patient-derived tumor. *Molecules* 2020;**25**:2362.
53. Krall N, Pretto F, Decurtins W, Bernardes GJL, Supuran CT, Neri D. A small-molecule drug conjugate for the treatment of carbonic anhydrase IX expressing tumors. *Angew Chem Int Ed* 2014;**53**:4231−5.
54. Cazzamalli S, Corso AD, Neri D. Linker stability influences the anti-tumor activity of acetazolamide–drug conjugates for the therapy of renal cell carcinoma. *J Control Release* 2017;**246**:39−45.
55. Marks IS, Gardeen SS, Kurdziel SJ, Nicolaou ST, Woods JE, Kularatne SA, et al. Development of a small molecule tubulysin b conjugate for treatment of carbonic anhydrase IX receptor expressing cancers. *Mol Pharm* 2018;**15**:2289−96.
56. Dudutienė V, Matulienė J, Smirnov A, Timm DD, Zubriene A, Baranauskiene L, et al. Discovery and characterization of novel selective inhibitors of carbonic anhydrase IX. *J Med Chem* 2014;**57**:9435−46.
57. Lv PC, Roy J, Putt KS, Low PS. Evaluation of nonpeptidic ligand conjugates for the treatment of hypoxic and carbonic anhydrase IX-expressing cancers. *Mol Cancer Therapeut* 2017;**16**:453.
58. Rami M, Winum JY, Innocenti A, Montero JL, Scozzafava A, Supuran CT. Carbonic anhydrase inhibitors: copper(II) complexes of polyamino-polycarboxylamido aromatic/heterocyclic sulfonamides are very potent inhibitors of the tumor-associated isoforms IX and XII. *Bioorg Med Chem Lett* 2008;**18**:836−41.
59. Janoniene A, Liu Z, Baranauskiene L, Makila E, Ma M, Salonen J, et al. A versatile carbonic anhydrase IX targeting ligand-functionalized porous silicon nanoplatform for dual hypoxia cancer therapy and imaging. *ACS Appl Mater Interfaces* 2017;**9**:13976−87.
60. Shabana AM, Mondal UK, Alam MR, Spoon T, Ross CA, Madesh M, et al. pH-Sensitive multiligand gold nanoplatform targeting carbonic anhydrase IX enhances the delivery of doxorubicin to hypoxic tumor spheroids and overcomes the hypoxia-induced chemoresistance. *ACS Appl Mater Interfaces* 2018;**10**:17792−808.
61. Alsaab HO, Sau S, Alzhrani RM, Cheriyan VT, Polin LA, Vaishampayan U, et al. Tumor hypoxia directed multimodal nanotherapy for overcoming drug resistance in renal cell carcinoma and reprogramming macrophages. *Biomaterials* 2018;**183**:280−94.
62. Tatiparti K, Rauf MA, Sau S, Iyer AK. A Biomimetic drug delivery system targeting tumor hypoxia in triple-negative breast cancers. *Appl Sci* 2020;**10**:1075.
63. Stiti M, Cecchi A, Rami M, Abdaoui M, Barragan-Montero V, Scozzafava A, et al. Carbonic anhydrase inhibitor coated gold nanoparticles selectively inhibit the tumor-associated isoform IX over the cytosolic isozymes I and II. *J Am Chem Soc* 2008;**130**:16130−1.
64. Bellissima F, Carta F, Innocenti A, Scozzafava A, Baglioni P, Supuran CT, et al. Structural modulation of the biological activity of gold nanoparticles functionalized with a carbonic anhydrase inhibitor. *Eur Phys J E Soft Matter* 2013;**36**:48.
65. Ratto F, Witort E, Tatini F, Centi S, Lazzeri L, Carta F, et al. Plasmonic particles that hit hypoxic cells. *Adv Funct Mater* 2015;**25**:316−23.
66. Ellis-Davies GCR. Caged compounds: photorelease technology for control of cellular chemistry and physiology. *Nat Methods* 2007;**4**:619.
67. Agasti SS, Chompoosor A, You CC, Ghosh P, Kim CK, Rotello VM. Photoregulated release of caged anticancer drugs from gold nanoparticles. *J Am Chem Soc* 2009;**131**:5728−9.
68. Barth A, Corrie JE. Characterization of a new caged proton capable of inducing large pH jumps. *Biophys J* 2002;**83**:2864−71.
69. Carbone M, Zlateva T, Quaroni L. Monitoring and manipulation of the pH of single cells using infrared spectromicroscopy and a molecular switch. *Biochim Biophys Acta Gen Subj* 2013;**1830**:2989−93.
70. Carbone M, Sabbatella G, Antonaroli S, Remita H, Orlando V, Biagioni S, et al. Exogenous control over intracellular acidification: enhancement *via* proton caged compounds coupled to gold nanoparticles. *Biochim Biophys Acta Gen Subj* 2015;**1850**:2304−7.
71. Sabbatella G, Antonaroli S, Diociauti M, Nucara A, Carbone M. Synthesis of proton caged disulphide compounds for gold nanoparticle functionalization. *New J Chem* 2015;**39**:2489−96.
72. Zhou L, Hu H, Zhang YX, Meng QY, Yu B, Shen YQ, et al. A near-infrared triggered intracellular pH regulative PAMAM/*O*-nitrobenzaldehyde coated UCNPs for cancer therapy. *Integrated Ferroelectrics Int J* 2019;**199**:85−94.
73. Lee ES, Na K, Bae YH. Polymeric micelle for tumor pH and folate-mediated targeting. *J Control Release* 2003;**91**:103−13.
74. Yin H, Lee ES, Kim D, Lee KH, Oh KT, Bae YH. Physicochemical characteristics of pH-sensitive poly(L-histidine)-*b*-poly(ethylene glycol)/poly(L-lactide)-*b*-poly(ethylene glycol) mixed micelles. *J Control Release* 2008;**126**:130−8.

75. Lee ES, Na K, Bae YH. Doxorubicin loaded pH-sensitive polymeric micelles for reversal of resistant MCF-7 tumor. *J Control Release* 2005;**103**:405−18.
76. Lee ES, Oh KT, Kim D, Youn YS, Bae YH. Tumor pH-responsive flower-like micelles of poly(L-lactic acid)-*b*-poly(ethylene glycol)-*b*-poly(L-histidine). *J Control Release* 2007;**123**:19−26.
77. Yin H, Kang HC, Huh KM, Bae YH. Biocompatible, pH-sensitive AB2 miktoarm polymer-based polymersomes: preparation, characterization, and acidic pH-activated nanostructural transformation. *J Mater Chem* 2012;**22**:19168−78.
78. Johnson RP, Uthaman S, John JV, Lee HR, Lee SJ, Park H, et al. Poly(PEGA)-*b*-poly(L-lysine)-*b*-poly(L-histidine) hybrid vesicles for tumoral pH-triggered intracellular delivery of doxorubicin hydrochloride. *ACS Appl Mater Interfaces* 2015;**7**:21770−9.
79. Hwang J-H, Choi CW, Kim H-W, Kim DH, Kwak TW, Lee HM, et al. Dextran-*b*-poly(L-histidine) copolymer nanoparticles for pH-responsive drug delivery to tumor cells. *Int J Nanomed* 2013;**8**:3197−207.
80. Lee ES, Kim JH, Sim T, Youn YS, Lee BJ, Oh YT, et al. A feasibility study of a pH sensitive nanomedicine using doxorubicin loaded poly(aspartic acid-*graft*-imidazole)-*block*-poly(ethylene glycol) micelles. *J Mater Chem B* 2014;**2**:1152−9.
81. Kim JH, Oh YT, Lee KS, Yun JM, Park BT, Oh KT. Development of a pH-sensitive polymer using poly(aspartic acid-*graft*-imidazole)-*block*-poly(ethylene glycol) for acidic pH targeting systems. *Macromol Res* 2011;**19**:453−60.
82. Ko J, Park K, Kim Y-S, Kim MS, Han JK, Kim K, et al. Tumoral acidic extracellular pH targeting of pH-responsive MPEG-poly(β-amino ester) block copolymer micelles for cancer therapy. *J Control Release* 2007;**123**:109−15.
83. Min KH, Kim J-H, Bae SM, Shin H, Kim MS, Park S, et al. Tumoral acidic pH-responsive MPEG-poly(β-amino ester) polymeric micelles for cancer targeting therapy. *J Control Release* 2010;**144**:259−66.
84. Lee JO, Oh KT, Kim D, Lee ES. pH-sensitive short worm-like micelles targeting tumors based on the extracellular pH. *J Mater Chem B* 2014;**2**:6363−70.
85. Wang J, Xu W, Guo H, Ding J, Chen J, Guan J, et al. Selective intracellular drug delivery from pH-responsive polyion complex micelle for enhanced malignancy suppression *in vivo*. *Colloids Surf B Biointerfaces* 2015;**135**:283−90.
86. Bilalis P, Tziveleka LA, Varlas S, Iatrou H. pH-Sensitive nanogates based on poly(L-histidine) for controlled drug release from mesoporous silica nanoparticles. *Polym Chem* 2016;**7**:1475−85.
87. Chen T, Wu W, Xiao H, Chen Y, Chen M, Li J. Intelligent drug delivery system based on mesoporous silica nanoparticles coated with an ultra-pH-sensitive gatekeeper and poly(ethylene glycol). *ACS Macro Lett* 2016;**5**:55−8.
88. Chen C, Yao W, Sun W, Guo T, Lv H, Wan X, et al. A self-targeting and controllable drug delivery system constituting mesoporous silica nanoparticles fabricated with a multi-stimuli responsive chitosan-based thin film layer. *Int J Biol Macromol* 2019;**122**:1090−9.
89. Uthaman S, Huh KM, Park I-K. Tumor microenvironment-responsive nanoparticles for cancer theragnostic applications. *Biomater Res* 2018;**22**:22.
90. Liao J, Zheng H, Fei Z, Lu B, Zheng H, Li D, et al. Tumor-targeting and pH-responsive nanoparticles from hyaluronic acid for the enhanced delivery of doxorubicin. *Int J Biol Macromol* 2018;**113**:737−47.
91. Zhang M, Liu J, Kuang Y, Ki Q, Zheng DW, Song Q, et al. Ingenious pH-sensitive dextran/mesoporous silica nanoparticles based drug delivery systems for controlled intracellular drug release. *Int J Biol Macromol* 2017;**98**:691−700.
92. Du J, Lane LA, Nie S. Stimuli-responsive nanoparticles for targeting the tumor microenvironment. *J Control Release* 2015;**219**:205−14.
93. Wu W, Luo L, Wang Y, Wu Q, Dai HB, Li JS, et al. Endogenous pH-responsive nanoparticles with programmable size changes for targeted tumor therapy and imaging applications. *Theranostics* 2018;**8**:3038−58.
94. Liu Y, Qiao L, Zhang S, Wan G, Chen B, Zhou P, et al. Dual pH-responsive multifunctional nanoparticles for targeted treatment of breast cancer by combining immunotherapy and chemotherapy. *Acta Biomater* 2018;**66**:310−24.
95. Wu W, Wang J, Lin Z, Li X, Li J. Tumor-acidity activated surface charge-conversion of polymeric nanocarriers for enhanced cell adhesion and targeted drug release. *Macromol Rapid Commun* 2014;**35**:1679−84.
96. Feng T, Ai X, An G, Yang P, Zhao Y. Charge-convertible carbon dots for imaging-guided drug delivery with enhanced *in vivo* cancer therapeutic efficiency. *ACS Nano* 2016;**10**:4410−20.
97. Hu J, Miura S, Na K, Bae YH. pH-responsive and charge shielded cationic micelle of poly(L-histidine)-*block*-short branched PEI for acidic cancer treatment. *J Control Release* 2013;**172**:69−76.
98. Ye G, Jiang Y, Yang X, Hu H, Wang B, Sun L, et al. Smart nanoparticles undergo phase transition for enhanced cellular uptake and subsequent intracellular drug release in a tumor microenvironment. *ACS Appl Mater Interfaces* 2018;**10**:278−89.
99. Du JZ, Sun TM, Song WJ, Wu J, Wang J. A Tumor-acidity-activated charge-conversional nanogel as an intelligent vehicle for promoted tumoral-cell uptake and drug delivery. *Angew Chem Int Ed* 2010;**49**:3621−6.
100. Yoon SR, Yang HM, Park CW, Lim S, Chung BH, Kim J-D. Charge-conversional poly(amino acid)s derivatives as a drug delivery carrier in response to the tumor environment. *J Biomed Mater Res* 2012;**100A**:2027−33.
101. Huang H, Li Y, Sa Z, Sun Y, Wang Y, Wang J. A Smart drug delivery system from charge-conversion polymer−drug conjugate for enhancing tumor therapy and tunable drug release. *Macromol Biosci* 2014;**14**:485−90.
102. Qu J, Peng S, Wang R, Yang ST, Zhou QH, Lin J. Stepwise pH-sensitive and biodegradable polypeptide hybrid micelles for enhanced cellular internalization and efficient nuclear drug delivery. *Colloids Surf B Biointerfaces* 2019;**181**:315−24.
103. Quan CY, Chen JX, Wang HY, Li C, Chang C, Zhang XZ, et al. Core−shell nanosized assemblies mediated by the $\alpha-\beta$ cyclodextrin dimer with a tumor-triggered targeting property. *ACS Nano* 2010;**4**:4211−9.
104. Zhang J, Yuan ZF, Wang Y, Chen WH, Luo GF, Cheng SX, et al. Multifunctional envelope-type mesoporous silica nanoparticles for tumor-triggered targeting drug delivery. *J Am Chem Soc* 2013;**135**:5068−73.
105. Pan J, Lei S, Chang L, Wan D. Smart pH-responsive nanoparticles in a model tumor microenvironment for enhanced cellular uptake. *J Mater Sci* 2019;**54**:1692−702.
106. Yang XZ, Du JZ, Dou S, Mao CQ, Long HY, Wang J. Sheddable ternary nanoparticles for tumor acidity-targeted siRNA delivery. *ACS Nano* 2012;**6**:771−81.
107. Fan M, Zeng Y, Ruan H, Zhang Z, Gong T, Sun X. Ternary nanoparticles with a sheddable shell efficiently deliver microRNA-34a against CD44-positive melanoma. *Mol Pharm* 2017;**14**:3152−63.
108. Li HJ, Du JZ, Liu J, Du XJ, Shen S, Zhu YH, et al. Smart superstructures with ultrahigh pH-sensitivity for targeting acidic tumor microenvironment: instantaneous size switching and improved tumor penetration. *ACS Nano* 2016;**10**:6753−61.
109. Li HJ, Du JZ, Du XJ, Xu CF, Sun CY, Wang HX, et al. Stimuli-responsive clustered nanoparticles for improved tumor penetration and therapeutic efficacy. *Proc Natl Acad Sci U S A* 2016;**113**:4164.
110. Anselmo AC, Mitragotri S. Nanoparticles in the clinic: an update. *Bioeng Transl Med* 2019;**4**:e10143.

111. Domenech M, Marrero-Berrios I, Torres-Lugo M, Rinaldi C. Lysosomal membrane permeabilization by targeted magnetic nanoparticles in alternating magnetic fields. *ACS Nano* 2013;**7**:5091−101.
112. Zhang E, Kircher MF, Koch M, Eliasson L, Goldberg SN, Renström E. Dynamic magnetic fields remote-control apoptosis *via* nanoparticle rotation. *ACS Nano* 2014;**8**:3192−201.
113. Cheng Y, Muroski ME, Petit DCMC, Mansell R, Vemulkar T, Morshed RA, et al. Rotating magnetic field induced oscillation of magnetic particles for *in vivo* mechanical destruction of malignant glioma. *J Control Release* 2016;**223**:75−84.
114. Shen Y, Wu C, Uyeda TQP, Plaza GR, Liu B, Han Y, et al. Elongated nanoparticle aggregates in cancer cells for mechanical destruction with low frequency rotating magnetic field. *Theranostics* 2017;**7**:1735−48.
115. Trapella C, Voltan R, Melloni E, Tisato V, Celeghini C, Bianco S, et al. Design, synthesis, and biological characterization of novel mitochondria targeted dichloroacetate-loaded compounds with anti-leukemic activity. *J Med Chem* 2016;**59**:147−56.
116. Misra SK, Ye M, Ostadhossein F, Pan D. Pro-haloacetate nanoparticles for efficient cancer therapy *via* pyruvate dehydrogenase kinase modulation. *Sci Rep* 2016;**6**:28196.
117. Yang Q, Cai J, Sun S, Kang X, Guo J, Zhu Y, et al. Polymer nanoparticle delivery of dichloroacetate and DACH-Pt to enhance antitumor efficacy and lower systemic toxicity. *Biomater Sci* 2016;**4**:661−9.
118. Bhat TA, Kumar S, Chaudhary AK, Yadav N, Chandra D. Restoration of mitochondria function as a target for cancer therapy. *Drug Discov Today* 2015;**20**:635−43.
119. Som A, Raliya R, Tian L, Akers W, Ippolit JE, Singamaneni S, et al. Monodispersed calcium carbonate nanoparticles modulate local pH and inhibit tumor growth *in vivo*. *Nanoscale* 2016;**8**:12639−47.
120. Som A, Raliya R, Paranandi K, High RA, Reed N, Beeman SC, et al. Calcium carbonate nanoparticles stimulate tumor metabolic reprogramming and modulate tumor metastasis. *Nanomedicine* 2019;**14**:169−82.